Published in The Plant Cell 21, issue 3, 767-785, 2009
which should be used for any reference to this work

Pheophytin Pheophorbide Hydrolase (Pheophytinase) Is Involved in Chlorophyll Breakdown during Leaf Senescence in *Arabidopsis* [W] [OA]

Silvia Schelbert,[a] Sylvain Aubry,[a,1] Bo Burla,[a,b] Birgit Agne,[c] Felix Kessler,[c] Karin Krupinska,[d] and Stefan Hörtensteiner[a,2]

[a] Institute of Plant Biology, University of Zürich, CH-8008 Zurich, Switzerland
[b] Postech-University of Zürich Global Research Laboratory Pohang, University of Science and Technology, Pohang, 790-784, Korea
[c] Laboratoire de Physiologie Végétale, Institut de Biologie, Université de Neuchâtel, CH-2009 Neuchâtel, Switzerland
[d] Institute of Botany and Central Microscopy, University of Kiel, D-24098 Kiel, Germany

During leaf senescence, chlorophyll is removed from thylakoid membranes and converted in a multistep pathway to colorless breakdown products that are stored in vacuoles. Dephytylation, an early step of this pathway, increases water solubility of the breakdown products. It is widely accepted that chlorophyll is converted into pheophorbide via chlorophyllide. However, chlorophyllase, which converts chlorophyll to chlorophyllide, was found not to be essential for dephytylation in *Arabidopsis thaliana*. Here, we identify pheophytinase (PPH), a chloroplast-located and senescence-induced hydrolase widely distributed in algae and land plants. In vitro, *Arabidopsis* PPH specifically dephytylates the Mg-free chlorophyll pigment, pheophytin (phein), yielding pheophorbide. An *Arabidopsis* mutant deficient in PPH (*pph-1*) is unable to degrade chlorophyll during senescence and therefore exhibits a stay-green phenotype. Furthermore, *pph-1* accumulates phein during senescence. Therefore, PPH is an important component of the chlorophyll breakdown machinery of senescent leaves, and we propose that the sequence of early chlorophyll catabolic reactions be revised. Removal of Mg most likely precedes dephytylation, resulting in the following order of early breakdown intermediates: chlorophyll → pheophytin → pheophorbide. Chlorophyllide, the last precursor of chlorophyll biosynthesis, is most likely not an intermediate of breakdown. Thus, chlorophyll anabolic and catabolic reactions are metabolically separated.

INTRODUCTION

Loss of green color is the most obvious sign of leaf senescence. A pathway of chlorophyll breakdown, comprising several enzymic reactions, has been elucidated in recent years (Hörtensteiner, 2006; Kräutler and Hörtensteiner, 2006). The early steps are localized in the chloroplast, but the final products of chlorophyll, linear tetrapyrrolic compounds termed nonfluorescent chlorophyll catabolites (NCCs) (Kräutler et al., 1991), are stored in the vacuole. The pathway starts with the removal of phytol and Mg by chlorophyllase (Willstätter and Stoll, 1913) and metal-chelating substance (Suzuki et al., 2005), respectively, before the porphyrin ring of the resulting intermediate, pheophorbide (pheide), is oxygenolytically opened by pheide *a* oxygenase (PAO) (Hörtensteiner et al., 1998). The product of this reaction is red chlorophyll catabolite, which, without release from PAO, is site-specifically reduced by red chlorophyll catabolite reductase to yield the primary fluorescent chlorophyll catabolite (FCC), pFCC (Mühlecker et al., 1997; Rodoni et al., 1997). After export from the chloroplast (Matile et al., 1992), pFCC is modified by reactions reminiscent of detoxification processes widely occurring in plants (Kreuz et al., 1996). Thus, pFCC is hydroxylated and after further (species-specific) modification (Kräutler, 2003; Hörtensteiner, 2006), the resulting FCCs are imported into the vacuole by a primary active transport process (Hinder et al., 1996). Finally, FCCs are converted to their respective NCCs by nonenzymatic tautomerization, catalyzed by the acidic vacuolar sap (Oberhuber et al., 2003). Structure analysis of NCCs from different plant species has revealed that, with one exception, they are all derived from chlorophyll *a* (Kräutler, 2003; Müller et al., 2006). A reason for this is the exclusive specificity of PAO for pheide *a* (Hörtensteiner et al., 1995), and it has been proposed that chlorophyll *b* to chlorophyll *a* conversion is a prerequisite for breakdown beyond the level of pheide (Hörtensteiner, 2006). It was suggested that decreasing the chlorophyll *b* portion in the chlorophyll-protein complexes of the photosystems causes their destabilization (Horn and Paulsen, 2004) and could trigger both apoprotein and chlorophyll degradation (Rüdiger, 2002; Hörtensteiner, 2006). This was corroborated recently by cloning of *NON-YELLOW COLORING1* (*NYC1*) and *NYC1-LIKE* (*NOL*) (Kusaba et al., 2007; Sato et al., 2009). *NYC1* and *NOL* encode two subunits of chlorophyll *b* reductase (Sato et al., 2009), which

[1] Current address: Department of Plant Sciences, University of Cambridge, Downing Street, Cambridge CB2 3EA, UK.
[2] Address correspondence to shorten@botinst.uzh.ch.
The author responsible for distribution of materials integral to the findings presented in this article in accordance with the policy described in the Instructions for Authors (www.plantcell.org) is: Stefan Hörtensteiner (shorten@botinst.uzh.ch).
[W] Online version contains Web-only data.
[OA] Open Access articles can be viewed online without a subscription.
www.plantcell.org/cgi/doi/10.1105/tpc.108.064089

catalyzes the first half of chlorophyll *b* to chlorophyll *a* reduction, i.e., conversion of chlorophyll *b* to 7-hydoxymethyl chlorophyll *a*. *nyc1* and *nol* mutants stay green during senescence and thereby selectively retain photosystem II (PSII) light-harvesting complex subunits (LHCII) and exhibit particularly high concentrations of chlorophyll *b*.

Mutants that retain greenness during senescence are collectively called stay-green mutants. Different types of stay-greens have been defined (Thomas and Howarth, 2000), and type C mutants were thought to be specifically impaired in chlorophyll catabolism, while other senescence-related processes proceed as normal. To date, three groups of type C stay-green mutants have been characterized, and their genetic lesion identified. Besides *nyc1/nol*, deficiency in the *PAO* gene was shown to cause a stay-green phenotype when senescence is induced in permanent darkness (Pružinská et al., 2005). In contrast with *nyc1*, *pao* mutants exhibit a lesion mimic phenotype under natural senescence, a consequence of the phototoxicity of the pheide *a* that accumulates in these mutants (Pružinská et al., 2003, 2005; Tanaka et al., 2003). Recently, a third group of type C stay-green mutants has become a major focus in plant senescence research. The best characterized of these mutants, Bf993 of *Festuca pratensis*, is defective in a gene now termed *stay-green* (*SGR*) (Thomas, 1987). *Festuca SGR* (Armstead et al., 2006, 2007) and orthologous genes have been molecularly identified from mutants of different species, such as *Arabidopsis thaliana* (*non yellowing1* [*nye1*]) (Ren et al., 2007), rice (*Oryza sativa*) (Jiang et al., 2007; Park et al., 2007; Sato et al., 2007), pea (*Pisum sativum*) (Sato et al., 2007; Aubry et al., 2008), bell pepper (*Capsicum annuum*) (Barry et al., 2008; Borovsky and Paran, 2008), and tomato (*Solanum lycopersicon*) (Barry et al., 2008). The *SGR* genes encode a family of novel chloroplast-located proteins, which most likely are required for chlorophyll-protein complex dismantling as a prerequisite for chlorophyll degrading enzymes to access their substrate (Park et al., 1998).

Chlorophyllase, which catalyzes the hydrolysis of chlorophyll to chlorophyllide (chlide) and phytol, was considered to be the rate-limiting step of the pathway (Takamiya et al., 2000; Harpaz-Saad et al., 2007). In 1999, chlorophyllase genes (termed *Chlase* or *CLH*) were cloned from orange fruit (*Citrus sinensis*) (Jakob-Wilk et al., 1999) as well as from Lamb's quarters (*Chenopodium album*) and *Arabidopsis* leaves (Tsuchiya et al., 1999), and further genes have been described since then (Hörtensteiner, 2006). Surprisingly, using well-established web-based programs, only some of these chlorophyllases were predicted to localize to the chloroplast, which led to the suggestion of alternative pathways of chlorophyll breakdown operating outside the plastid (Takamiya et al., 2000), or questioned the involvement of CLHs in chlorophyll breakdown (Hörtensteiner, 2006). Recently, it was shown that the two *Arabidopsis* chlorophyllases (CLH1 and CLH2) are not essential for in vivo chlorophyll breakdown during leaf senescence (Schenk et al., 2007).

Here, we report the identification of candidates for chlorophyll dephytylation based on a functional genomic approach that considers features expected for such a hydrolase, including senescence-related regulation and chloroplast localization. In the course of our investigations, we show that one of the candidate genes (At5g13800) encodes a pheophytin (phein = Mg-free chlorophyll) hydrolase. We therefore named At5g13800 pheophytinase (PPH). *PPH* mutants, termed *pph*, exhibit a type C stay-green phenotype during senescence. *pph-1* retains thylakoid ultrastructure and photosystem protein subcomplexes. Heterologously expressed PPH dephytylates phein to pheide but does not accept chlorophyll as substrate. Small but significant quantities of phein *a* are found in *pph-1*, indicating that also in vivo, PPH functions as a phein hydrolase. PPH orthologs are present in different higher plant genomes, indicating an important function. Collectively, we identified a likely candidate for porphyrin-phytol hydrolysis involved in senescence-related chlorophyll breakdown in vivo. The enzyme is active on phein but not chlorophyll. We therefore propose that the early reactions of chlorophyll breakdown in leaves proceed in the following order: chlorophyll *b* → chlorophyll *a* → phein *a* → pheide *a*.

RESULTS

Identification of Possible Phytol-Hydrolyzing Proteins in *Arabidopsis*

Biochemical and molecular analysis of chlorophyll breakdown together with structure elucidation of FCCs and NCCs had indicated that pigment dephytylation is an early reaction of the pathway most likely occurring inside the chloroplast (Hörtensteiner, 2006). Chemically, phytol cleavage is an ester hydrolysis reaction; thus, candidate proteins, like most esterases and lipases (Fojan et al., 2000), likely contain an α/β hydrolase fold. Using The Arabidopsis Information Resource (TAIR) *Arabidopsis* genome annotation (release 8), we screened for proteins whose descriptions contained the phrase "alpha/beta" (Figure 1A). Of the resulting 462 proteins, 42 were predicted by ChloroP (Emanuelsson et al., 1999) to localize to the chloroplast. No function had yet been assigned for 30 of these proteins belonging to 24 gene loci. Similar to other genes involved in chlorophyll catabolism (*SGR1*, *NYC1*, and *PAO*), expression of the candidates was expected to be rather high during senescence. According to microarray expression data of the 24 candidate genes (Zimmermann et al., 2004), three genes, namely, At1g54570, At3g26840, and At5g13800, showed a leaf senescence-related expression pattern (Figure 1B). We focused on these genes and analyzed respective T-DNA insertion mutants. These were obtained from the SALK resource (Alonso et al., 2003) (*at1g54570-1*, SALK_034549; *at3g26840-1*, SALK_071769; and *at5g13800-1* [*pph-1*], SALK_000095), and homozygous progeny were identified by PCR. Since At1g54570 and At3g26840 are homologous genes that could have redundant function, we also produced an *at1g54570-1 at3g26840-1* double knockout line. When detached leaves were incubated in darkness to induce senescence, all lines except *at5g13800-1* degraded chlorophyll like the wild type (Figure 1C). Thus, absence of At5g13800 caused a stay-green phenotype. In addition, *At5g13800* expression was highly correlated with *PAO* expression when analyzing coexpression with web-based analysis tools (http://www.Arabidopsis.leeds.ac.uk/act/coexpanalyser.php; http://csbdb.mpimp-golm.mpg.de/csbdb/dbcor/ath.html). We concluded that At5g13800 might be a genuine chlorophyllase, but in the course of our investigations

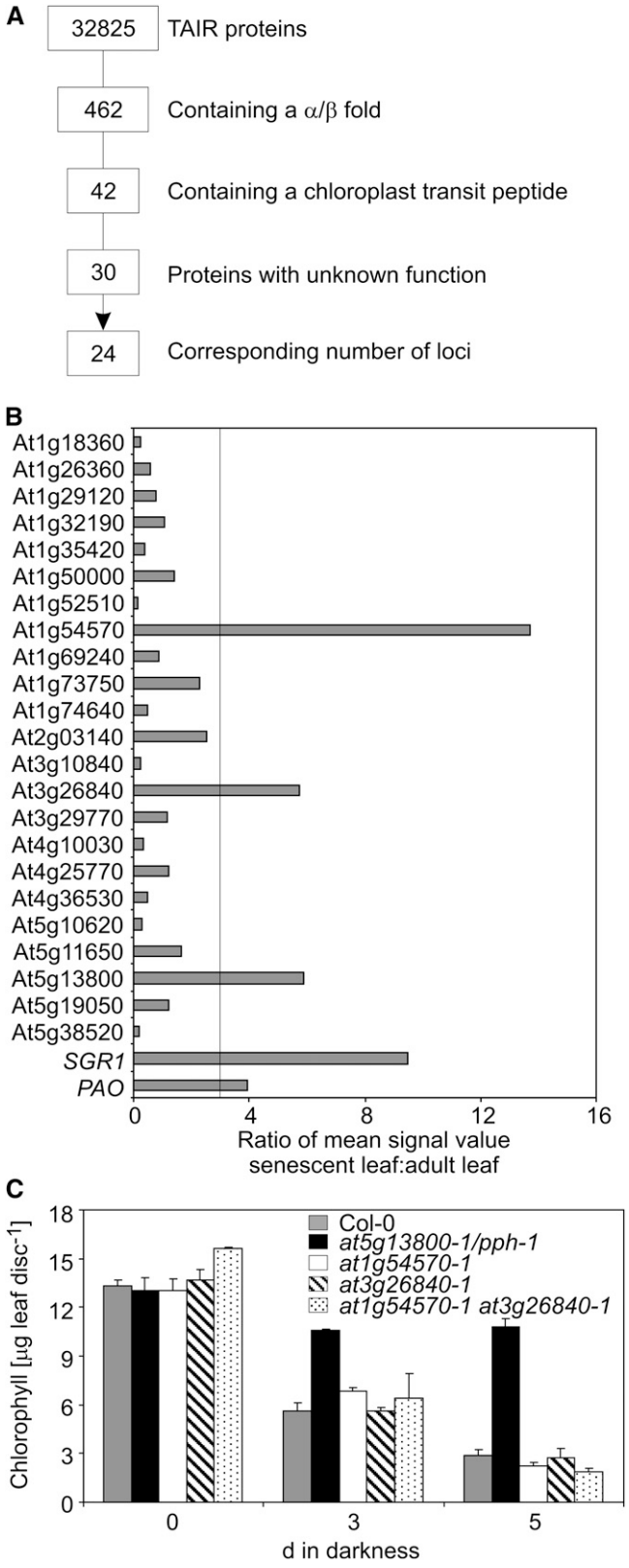

Figure 1. Identification and Analysis of Candidates for Phytol Hydrolysis in *Arabidopsis*.

identified that the enzyme specifically hydrolyzed the phytolester of phein but not chlorophyll (see below). We therefore named At5g13800 PPH and focused on analyzing respective *pph* mutants.

PPH Deficiency Results in a Stay-Green Phenotype

Microarray data analyzed by Genevestigator (Zimmermann et al., 2004) indicated enhanced *PPH* expression during leaf senescence (Figure 1B). We confirmed this by RT-PCR analysis of the wild type (Figure 2B). To confirm that absence of PPH was responsible for the stay-green phenotype observed in *at5g13800-1* (*pph-1*) (Figure 1C), two additional homozygous T-DNA insertion lines for At5g13800, namely, *pph-2* (GABI_453A08) and *pph-3* (SM_3_15198) (Figure 2A), were analyzed. In all cases, high levels of chlorophyll were retained during natural (see Supplemental Figure 1 online) and dark-induced senescence (Figures 2C and 2D), and *pph-1* was exclusively used in our subsequent studies. Furthermore, we introduced *PPH* cDNA into *pph-1* under the control of the 35S promoter. The stay-green phenotype was complemented in *pph-1/35S:PPH* plants (i.e., upon dark-induced senescence, chlorophyll was degraded like in the wild type) (Figure 2E). Complementation depended on the presence of the Ser-221 residue of *Arabidopsis* PPH, which possibly represents the active site residue (see below). Thus, *pph-1/35S:PPH*$_{S221A}$ lines retained indefinite greenness. Altogether the data indicated that *PPH* absence causes a stay-green phenotype during leaf senescence.

pph-1 Is a Type C Stay-Green Mutant

Stay-green mutants have been classified into functional stay-greens, in which both chlorophyll degradation and photosynthetic capacity are retained longer compared with the wild type, and cosmetic ones (e.g., type C), which specifically retain chlorophyll while other senescence parameters are not affected (Thomas and Howarth, 2000). To examine the correlation between greenness and leaf functionality in *pph-1*, we determined the maximal fluorescence yield of PSII (F_v/F_m) (Figure 3A) and CO_2 consumption in correlation to light intensities (see Supplemental Figure 2 online). For these experiments, senescence was induced by covering attached leaves with aluminum foil. F_v/F_m decreased more rapidly in *pph-1* than in the wild type. Likewise,

(A) Screening of the TAIR protein database (version 8) for proteins with properties expected for a phytol-hydrolyzing enzyme.

(B) Analysis of senescence-related expression of candidate genes using the Genevestigator Meta-Analyzer tool (Zimmermann et al., 2004). The ratio of mean fluorescence values from senescent leaves (organ #44, number of chips: 3) and adult leaves (organ #42, number of chips: 274) is shown. Values for *SGR1* and *PAO* are shown as reference. A cutoff of 3 was chosen for significantly upregulated genes. Note that one of the 24 candidate genes (At5g47860) was not present on the 22K microarray chip.

(C) Degradation of chlorophyll during dark-induced senescence in mutants of candidate genes. Data are mean values of a representative experiment with three technical replicates. Error bars indicate SD.

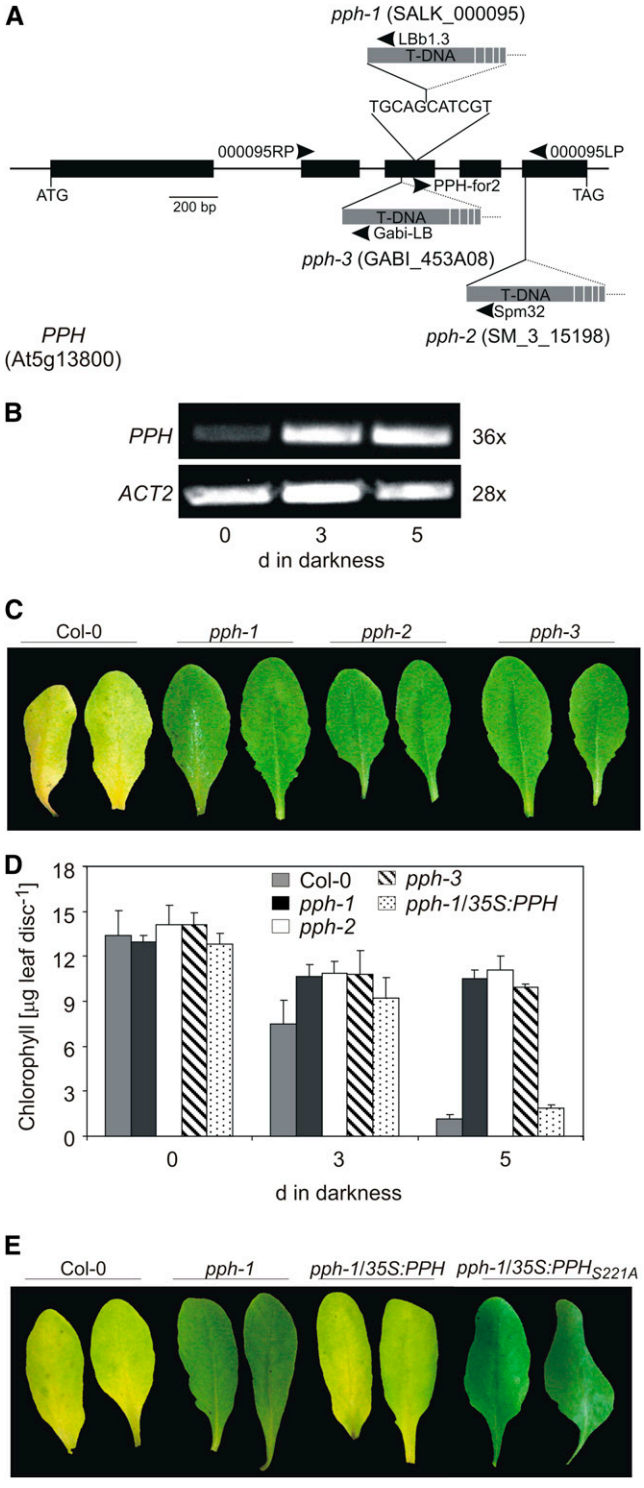

Figure 2. Deficiency of PPH Causes a Stay-Green Phenotype.

(A) Gene structure of *PPH* showing the T-DNA insertion sites of the different *pph* mutants studied here. For *pph-1*, the site of T-DNA insertion was verified by sequencing. Position of primers used for isolation of homozygous lines is shown.

(B) Analysis of *PPH* expression during dark-induced senescence. *ACT2* was used as control. Expression was analyzed with nonsaturating numbers of PCR cycles as shown at the right. The results from one of three independent experiments with similar results are shown. PCR products were separated on agarose gels and visualized with ethidium bromide.

(C) Phenotype of three *pph* mutants after 5 d of dark-induced senescence.

(D) Chlorophyll degradation of *pph* mutants and *pph-1* complemented with a *35S-PPH* cDNA construct (*pph-1/35S:PPH*) during dark-induced senescence. Data are mean values of a representative experiment with three replicates. Error bars indicate SD.

(E) Complementation of the stay-green phenotype of *pph-1* with a *35S-PPH* cDNA construct. A construct harboring a mutation of the proposed active-site Ser residue (*35S-PPH*$_{S221A}$) did not complement *pph-1*. Leaves after 5 d of dark-induced senescence are shown.

CO_2 fixation rates decreased faster in *pph-1* (see Supplemental Figure 2 online), demonstrating that functionality of photosynthesis was strongly affected in *pph-1* upon senescence induction. To further characterize the senescence behavior of *pph-1*, expression of *SAG12*, a commonly accepted marker of senescence, was analyzed by RT-PCR (Figure 3B). In both the wild type and *pph-1* mutant, *SAG12* expression increased to a similar extent upon senescence induction. In addition, senescence-regulated genes of chlorophyll degradation (i.e., *NYC1*, *SGR1*, and *PAO*) were induced in *pph-1* (Figure 3B), indicating that chlorophyll was retained in the mutant despite the induction of the chlorophyll degradation pathway. We analyzed metabolism of photosynthesis-related proteins as a further marker of senescence progression (Figure 3C). As had been shown in other instances of type C stay-green mutants (Thomas and Hilditch, 1987; Pružinská et al., 2003; Kusaba et al., 2007; Park et al., 2007), degradation of LHC subunits was delayed in *pph-1*, while ribulose-1,5-bisphosphate carboxylase/oxygenase (Rubisco) was degraded like in the wild type. In addition, PsbA (D1), a subunit of the core complex of PSII, was also partially retained in *pph-1*. By contrast, PsaA degradation in *pph-1* was indistinguishable from that of the wild type. Collectively, these data showed that *pph-1* is a type C stay-green mutant specifically impaired in chlorophyll catabolism.

PPH Is Required for Chloroplast and Photosystem Degradation

Type C stay-green mutants are characterized by an increased stability of chloroplast membranes and of chlorophyll-protein complexes (Kusaba et al., 2007; Park et al., 2007; Sato et al., 2007). Ultrastructural analysis showed that chloroplast structure of short day-grown *pph-1* plants was similar to that of the wild type before senescence (Figure 4A). After 6 d of dark-induced senescence, grana thylakoid stacking in *pph-1* was nearly unchanged. In some cases, stacks with significantly more lamellae per granum were present, probably due to fusion of several grana stacks as reported earlier (Kusaba et al., 2007). By contrast, in the wild type, grana were largely unstacked and overall thylakoid membrane density was reduced. This indicated that PPH absence prevented proper degradation of the thylakoid membrane

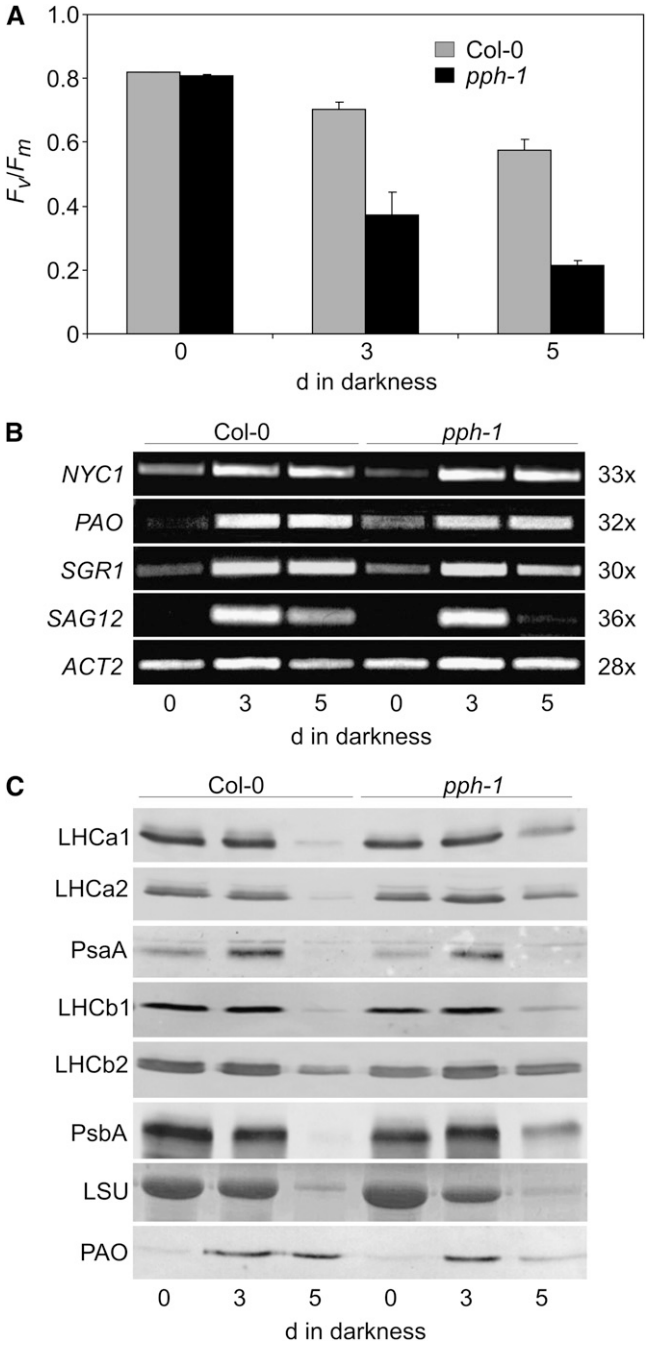

Figure 3. Characterization of Senescence Parameters in *pph-1*.

(A) Maximum quantum yield of PSII (F_v/F_m) during senescence in Col-0 (gray) and *pph-1* (black). For senescence induction, attached leaves were covered with aluminum foil. Data are mean values of a representative experiment with three to six replicates. Error bars indicate SE.

(B) Analysis of gene expression during dark-induced senescence in Col-0 and *pph-1*. *ACT2* was used as control. Expression was analyzed with nonsaturating numbers of PCR cycles as shown at the right. The results from one of two independent experiments with similar results are shown. PCR products were separated on agarose gels and visualized with ethidium bromide.

(C) Immunoblot analysis of degradation of photosynthesis-related proteins during dark-induced senescence in Col-0 and *pph-1*. PAO was used as a marker for senescence induction. Gel loadings are based on equal size of leaf area. LSU, Rubisco large subunit.

system. To further analyze composition and stability of photosystem subcomplexes, isolated and mildly solubilized chloroplast membranes were separated by sucrose density gradient centrifugation (Figure 4B; see Supplemental Figure 3 online). In *pph-1*, the photosynthetic complex structure remained largely unchanged upon senescence induction. By contrast, all complexes were degraded in the wild type. Immunoanalysis of sucrose density gradient fractions indicated that after 5 d of dark-induced senescence, the LHCII and PSII core complexes formed bands at lower densities in both the wild type and *pph-1* (see Supplemental Figure 3 online). This occurred reproducibly in several independent experiments, possibly due to changes in ultrastructural composition of respective complexes or altered detergent solubilization properties. Furthermore, as seen before (Figure 3C), PsaA was degraded in both lines, while the abundance of all other subunits analyzed by immunoblots remained largely unchanged in *pph-1* (see Supplemental Figure 3 online).

PPH Is Localized in the Chloroplast

The above-described chloroplast metabolism-related phenotype of *pph-1* indicated localization of PPH inside the chloroplast. Furthermore, ChloroP predicted the presence in PPH of a N-terminal chloroplast transit peptide of 46 amino acids. An N-terminal fusion with PPH (PPH-GFP) targeted green fluorescent protein (GFP) to the chloroplasts of *Arabidopsis* mesophyll protoplasts (Figure 5A). Thereby, GFP fluorescence largely colocalized with chlorophyll fluorescence. By contrast, GFP fusions with translocon of the inner chloroplast envelope110 (TIC110) resulted in distinct chlorophyll and GFP fluorescences as expected (Schenk et al., 2007), indicating envelope localization. In addition, we performed import experiments of [^{35}S]-labeled PPH into isolated *Arabidopsis* mesophyll chloroplasts, followed by chloroplast reisolation and subfractionation (Figure 5B). PPH was efficiently imported into the plastids and was found in the soluble fraction. From these experiments, we conclude that PPH is located inside the chloroplast, most likely as a soluble protein in the stroma.

pph-1 Has a Defect in Chlorophyll Degradation and Accumulates Pheophytin *a*

Different stay-green mutants have been shown to accumulate green intermediates of chlorophyll breakdown (i.e., chlide and/or pheide) (Roca et al., 2004; Park et al., 2007). To investigate the pigment composition in *pph-1* during senescence, green pigments were extracted and separated by reverse-phase HPLC (Figure 6A). Before senescence, the wild type and *pph-1* were indistinguishable, and after 5 d of dark-induced senescence, chlorophyll *a* and chlorophyll *b* levels diminished in the wild type (Figure 6A). By contrast, in *pph-1*, large quantities of chlorophyll *a*

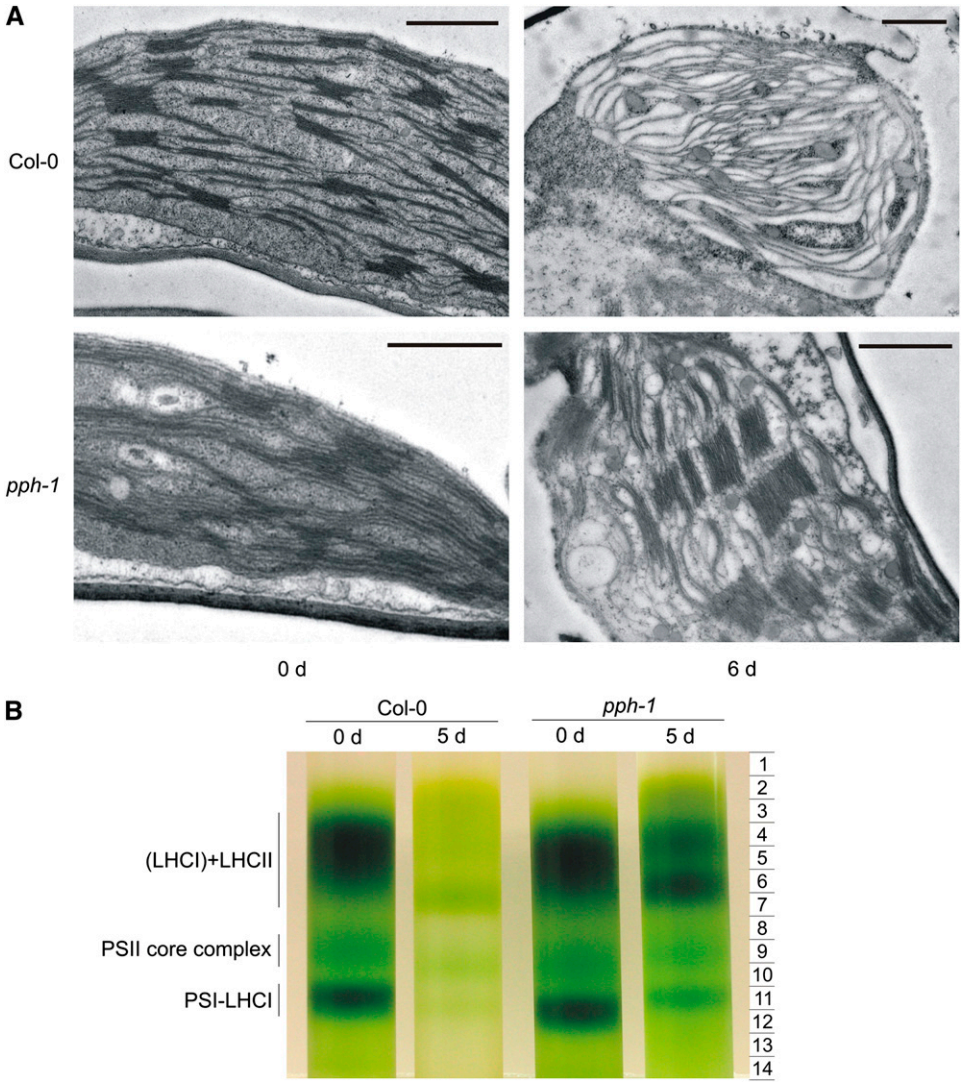

Figure 4. Analysis of Photosystem Organization During Senescence in *pph-1*.

(A) Transmission electron micrographs of plastids from short-day-grown Col-0 and *pph-1* before (0 d) and after 6 d of dark-induced senescence. Bars = 1 μm.

(B) Sucrose gradient fractionation of thylakoid membranes from Col-0 and *pph-1* before (0 d) and after 5 d of dark-induced senescence. Dodecylmaltoside-solubilized thylakoid membranes corresponding to equal amounts of fresh weight were loaded on each gradient. Gradient fractions (1 to 14) used for further analysis are shown at the right. The position of photosystem subcomplexes, as identified by immunoblot analysis of individual photosystem subunits (see Supplemental Figure 3 online), is indicated at the left. Note that during senescence, the LHCII band separated into two distinct bands in both Col-0 and *pph-1*.

and in particular chlorophyll *b* were retained (Figure 6B), with the result that the chlorophyll *a*/*b* ratio decreased during senescence (Figure 6C). This occurred in three different *pph* mutants. When plants had been grown under strong light, significant quantities of chlorophyll *a* were converted to C_{13}-hydroxy chlorophyll *a*, and two additional minor chlorophyll *a*-like peaks formed upon senescence induction in *pph-1*, but not in Columbia-0 (Col-0) (see Supplemental Figure 4 online). Production of these modified pigments could be induced in the wild type and the mutant by treatment with H_2O_2 (see Supplemental Figure 4 online), indicating that their formation was due to (unspecific) peroxidative activities.

pph-1 accumulated increasing amounts of phein *a* (Figure 6D) after 3 and 5 d of dark-induced senescence. This was not seen in the wild type, indicating that absence of PPH in the mutant was responsible for the observed phein accumulation. To investigate the possibility that phein accumulation in *pph-1* could be limited by some capacity on the part of PAO to cause conversion of phein *a* to an FCC-like pigment, we produced a *pph-1 pao1* double mutant. We found that phein *a* accumulation in *pph-1 pao1* was

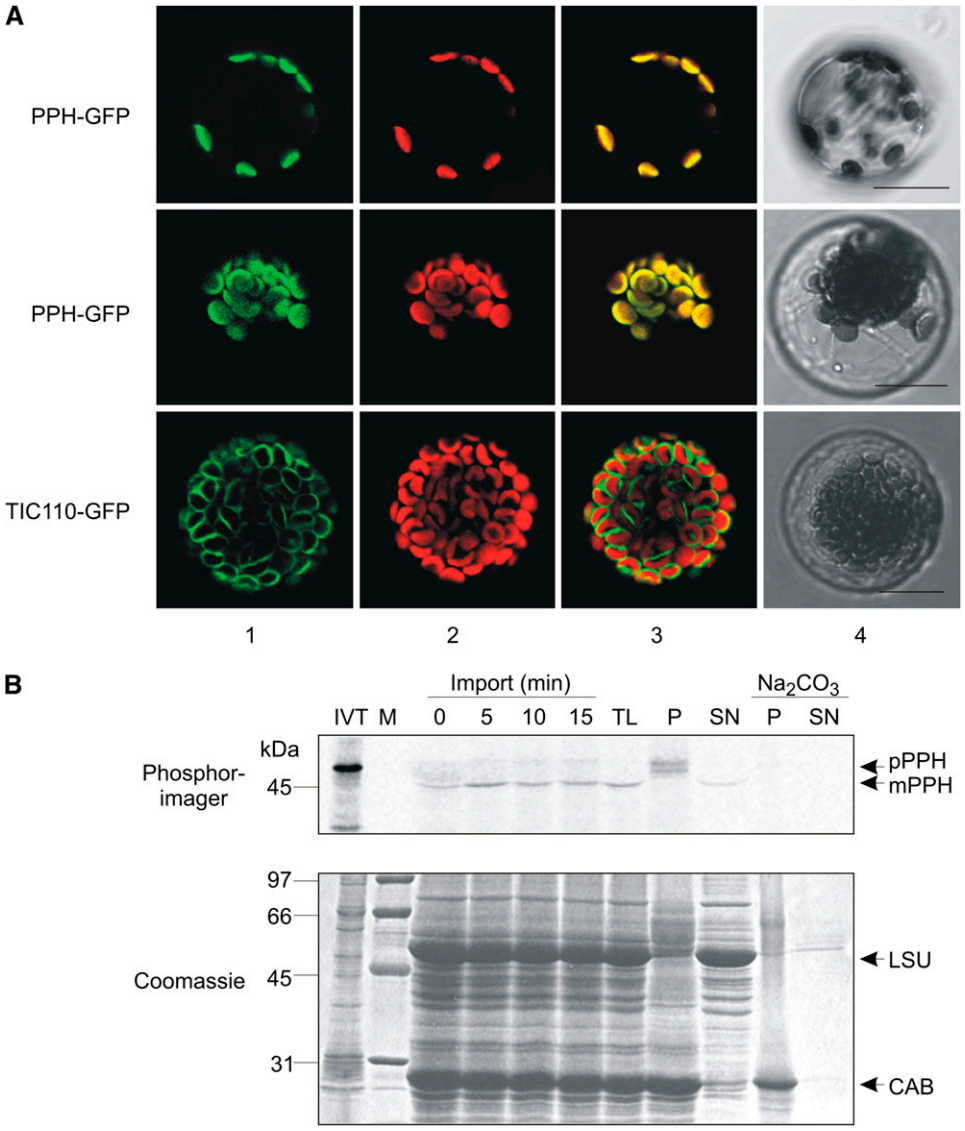

Figure 5. Analysis of Subcellular PPH Localization.

(A) Transient expression in *Arabidopsis* mesophyll protoplasts of GFP fused in frame to the C terminus of PPH (PPH-GFP). TIC110-GFP was used as control for chloroplast envelope localization. GFP fluorescence (column 1) and chlorophyll autofluorescence (column 2) were examined by confocal laser scanning microscopy. Column 3, merge of GFP and autofluorescence; column 4, bright field image. Bars = 10 μm.

(B) Import of [^{35}S]-Met–labeled precursor of PPH (pPPH) in *Arabidopsis* chloroplasts. Import was allowed to proceed for 5, 10, and 15 min and mature PPH (mPPH) accumulated. After 15 min of import, chloroplasts were treated with thermolysin (TL) to digest surface-bound and nonimported precursor. To determine the subchloroplast PPH localization, chloroplasts were lysed and separated into stromal (SN) and membrane (P) fractions. The membrane fraction was subjected to alkaline extraction (Na_2CO_3) and separated into Na_2CO_3-resistant proteins (P) or proteins extractable by this treatment (SN). M, molecular size markers (kD) are indicated at the left. IVT, in vitro translation product; LSU, large subunit of Rubisco; CAB, chlorophyll *a*/*b* binding protein.

similar to that in *pph-1* (Figure 6D). Only small amounts of polar NCCs (i.e., linear tetrapyrroles known as late products of chlorophyll breakdown in *Arabidopsis* [Pružinská et al., 2005]) were found in *pph-1* (Figure 6E), indicating that, in *pph-1*, chlorophyll breakdown was largely blocked at the level of porphyrinic, phytol-containing pigments.

PPH Is a Pheophytinase (PPH)

To investigate the enzymatic activity of PPH, a truncated version, devoid of the predicted chloroplast transit peptide (ΔPPH), was expressed in *Escherichia coli* as a maltose binding protein (MBP) fusion (MBP-ΔPPH). The recombinant protein was highly stable

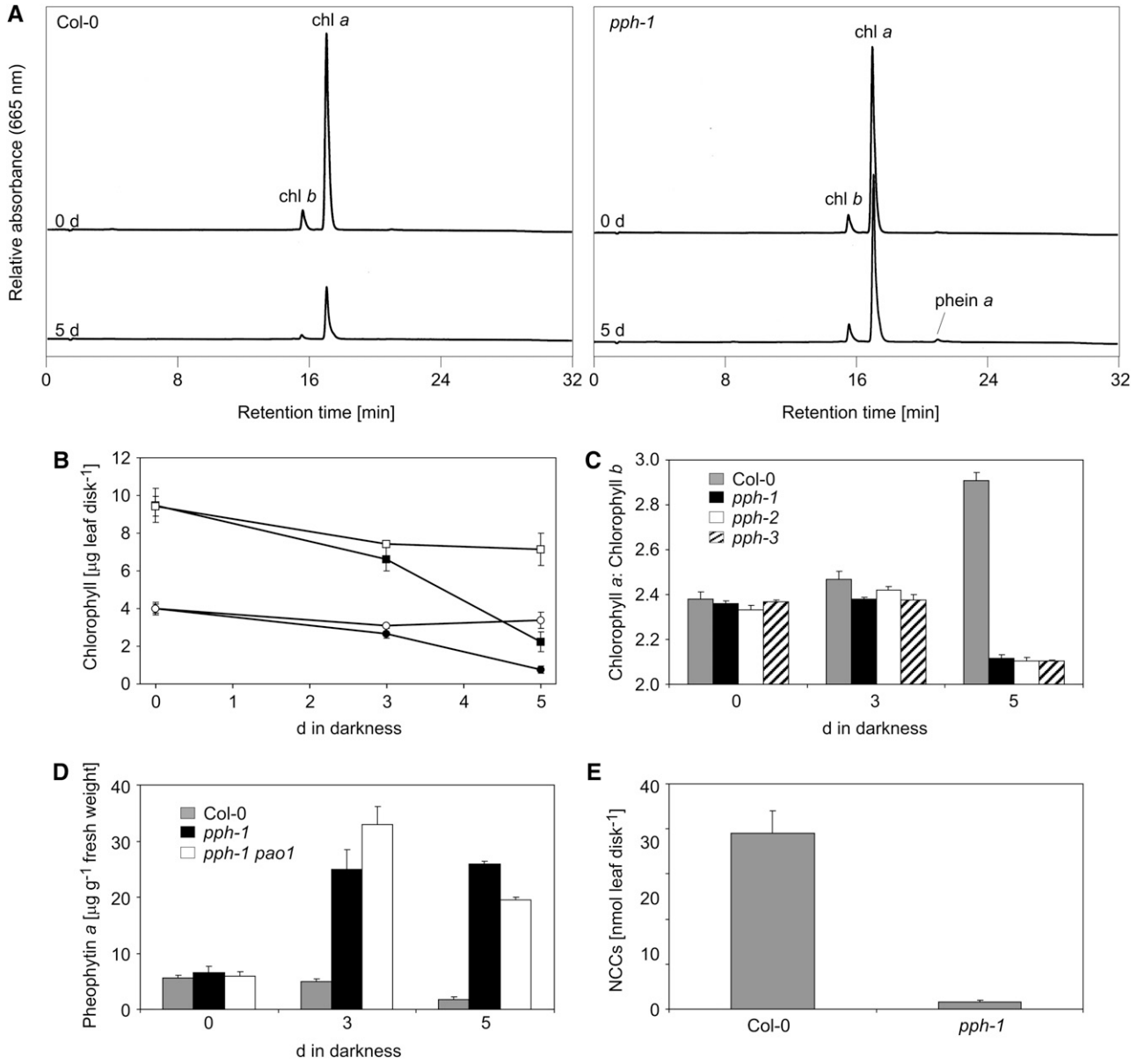

Figure 6. Analysis of Pigment Composition during Dark-Induced Senescence in *pph-1*.

(A) HPLC traces (A_{665}) of leaf extracts of Col-0 (left) and *pph-1* (right) before (0 d) and after 5 d of senescence. HPLC injections correspond to equal amounts of fresh weight. Chl, chlorophyll.

(B) Degradation of chlorophyll *a* (squares) and chlorophyll *b* (circles) during senescence of Col-0 (closed) and *pph-1* (open).

(C) Ratio of chlorophyll *a* to chlorophyll *b* during senescence of Col-0 and different *pph* mutants.

(D) Amounts of phein *a* (pheophytin *a*) accumulating during senescence in Col-0 (gray), *pph-1* (black), and *pph-1 pao1* (white).

(E) Amount of total NCCs found in Col-0 and *pph-1* after 5 d of dark-induced senescence.

Data in **(B)** to **(E)** are mean values ± SD of representative experiments each with three replicates.

and was largely located in the soluble cell fraction (Figure 7A). Crude soluble *E. coli* extracts were employed in assays containing chlorophyll *a*/*b* mixtures as likely substrates. MBP-ΔPPH did not convert chlorophyll to chlide (Figure 7B), in contrast with recombinant *Citrus* chlorophyllase (Chlase1), which was highly active (see Supplemental Figure 5A online). Since phein accumulated in *pph-1* (Figure 6D), we explored the possibility of the Mg-free pigment being a substrate of PPH. Indeed, MBP-ΔPPH (Figure 7C) converted phein to the respective dephytylated pigment, pheide, thereby reacting with both phein *a* and phein *b* (Figures 7C and 7D). Activity was identical before and after cleavage of the fusion protein with factor XA (see Supplemental

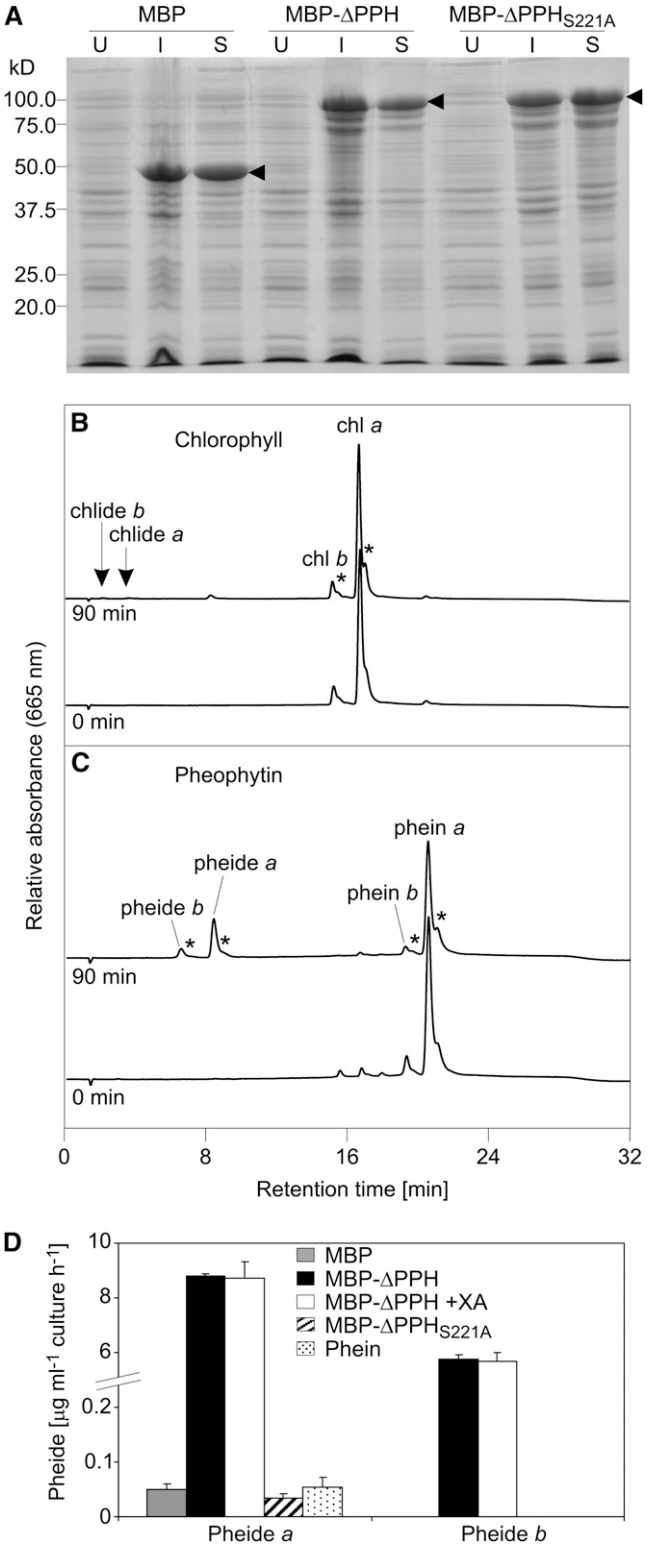

Figure 7. Analysis of Recombinant and Native PPH.

(A) Coomassie blue–stained SDS-PAGE gel of *E. coli* cells (BL21 DE3) expressing an N-terminal truncated version of PPH (ΔPPH) fused to MBP (MBP-ΔPPH). In addition, a missense mutation of PPH (MBP-ΔPPH$_{S221A}$) was analyzed. A strain expressing free MBP was used as control. After induction with isopropyl-β-D-thiogalactopyranosid for 3 h (I), cells were lysed, and soluble proteins (S) were isolated as described in Methods. U, cells before isopropyl-β-D-thiogalactopyranosid induction. Gel loadings are based on equal amounts of cell cultures at OD_{600} = 1.5. Arrowheads indicate position of recombinant proteins. Molecular size markers (kD) are indicated at the left.

(B) and **(C)** HPLC analysis of assays employing soluble *E. coli* lysates expressing recombinant MBP-ΔPPH with chlorophyll **(B)** or phein **(C)** as substrate. HPLC traces at A_{665} before (0 min) and after 90 min of incubation at 25°C are shown. Note that only in the case of phein were the respective dephytylated products (pheides) formed. Asterisks indicate the C_{13} epimers of adjacent peaks. In **(B)**, arrows indicate the expected position of chlide *b* and chlide *a*, respectively. Chl, chlorophyll.

(D) Pheide *a* (left) and pheide *b* (right) formation from phein in assays with recombinant MBP-ΔPPH before (black) and after (white) 24 h of digestion with factor XA. As controls, the substrate was incubated with the vector control (MBP, gray), recombinant MBP-ΔPPH$_{S221A}$ (hatched), or without *E. coli* extract (Phein; dotted). Data are mean ± SD of three independent assays.

Figure 6C online; Figure 7D), and *E. coli* extracts containing the uncut MBP-ΔPPH fusion were employed in subsequent assays. In competition experiments, a 10-fold excess of chlorophyll did not inhibit phein hydolysis. Thus, PPH exhibited a surprising specificity for the Mg-free form of chlorophyll, in contrast with *Citrus* Chlase1, which catalyzed dephytylation of both chlorophyll and phein (see Supplemental Figures 5A and 5B online). While chlorophyllase showed the known specificity (Fiedor et al., 1992) toward *a* and *b* forms of pigments and did not react with the respective C_{13} epimers (see Supplemental Figures 5A and 5B online), PPH accepted both C_{13} epimers of phein *a* and phein *b* (Figure 7C). The phein hydrolytic activity of recombinant MBP-ΔPPH was time dependent and exhibited a temperature optimum of 25 to 30°C (see Supplemental Figure 6 online). Neither the vector control nor the mutation of a Ser residue (Ser-221), possibly representing the active site residue of *Arabidopsis* PPH (MBP-ΔPPH$_{S221A}$), acted on phein (Figure 7D) or chlorophyll.

PPH Is a Ser-Type Hydrolase Widely Distributed in Eukaryotic Photosynthetic Organisms

BLASTP searches (Altschul et al., 1997) for homologous PPH proteins using databases at the National Center for Biotechnology Information and the Joint Genome Institute identified PPH-related proteins from higher and lower plant species and from cyanobacteria. To investigate the relationship between these proteins, we performed a phylogenetic analysis on selected proteins within the BLAST hits. We included all nonredundant eukaryotic proteins, but for better visibility, left out bacterial species, except for proteins from *Synechocystis* sp PCC6803 and *Synechococcus* sp PCC7002 (Figure 8A; see Supplemental Data Set 1 online). *Arabidopsis* PPH clustered into a clade (clade I) with one protein each from eukaryotic plant species included in the analysis, but not with bacterial sequences. Two further clades (clade II and III), clearly separated from clade I, were obtained. This indicated that PPH orthologs are commonly present in eukaryotic photosynthesizing organisms, but absent in cyanobacteria. The distribution within the tree further indicated

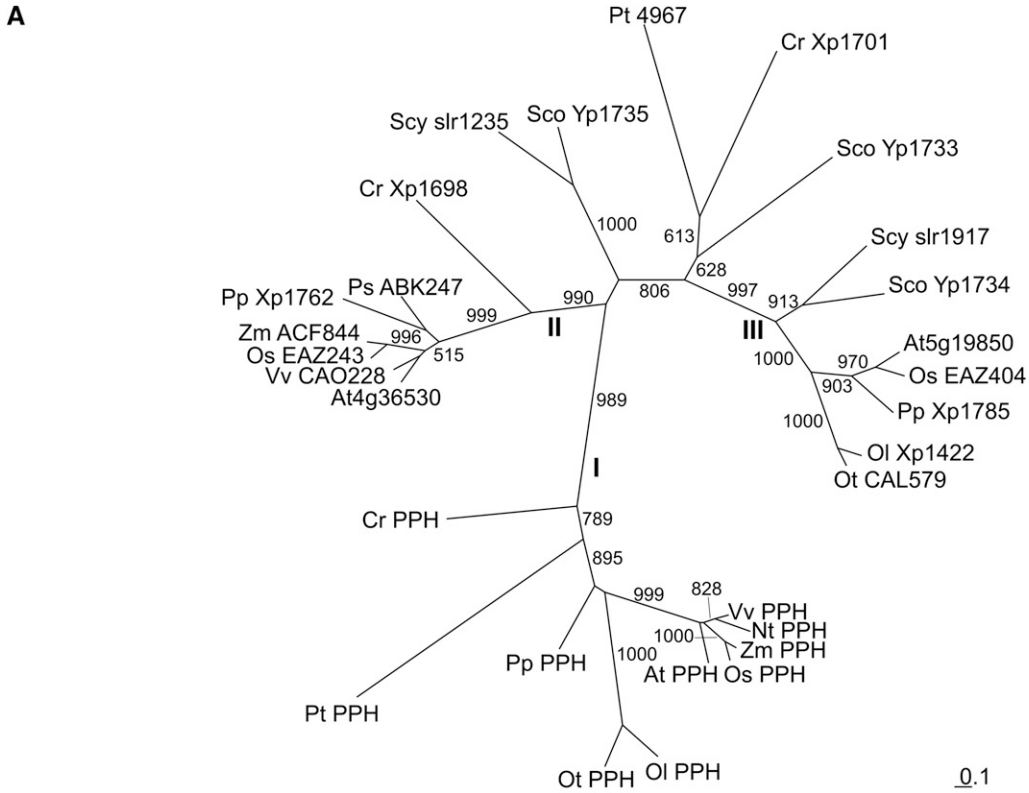

B

```
                 *        20        *        40        *        60        *        80        *
At PPH : MEIISLNVVPQCSVVTWS--SKLATKRLVPNRSSLLFSGVKKSRLVIR-------------------------------------------- :  46
Vv PPH : MEILSCHSAPCCKLVNLG--GTSVHKSSGSSQAKLPGSFNNRILCARIGSKLGSSGYSNLDDFCTKNFGRHEGSRSLTAFKGSANVNSKA :  88
Os PPH : MEVVSSSHSCLAFNRTPSSAWRFPGNGLGPGHAKLTRPRSA-ILCVRSGT---ASNPA---------------------------DSGK :  58
Zm PPH : MEVVSCSHSCSALHQTPASTWRLRGSALGLGLGHARPSRTRRYTVACVGTTSGASNPG---------------------------GSGK :  62
Ot PPH : ------------------------------------------------------------------------------------------ :   -

                100       *       120       *       140       *       160       *       180
At PPH : -SGNSDGYVVGENDDLGRIAR-RGESTSKVLIPGLPDESNGEIAARISHSHCEWKPKLRVHYEKAGCDNLDAPAVLFLPGFGVGSFHYEK : 134
Vv PPH : LSESYNGYVIDGKEGVGDISE-RGDLITQILIPGLPDDSNDDSGAQISSCFWEWKPKLTVHYEKSGCENVNSPPVLFLPGFGVGSFHYEK : 177
Os PPH : VHASHGFYVSDVDAALQGIPK-KVGEIEKMIIPSLPE---GPESSLISTGFWEWKPKLSVYYEKSGIDNSKAPSVLFLPGFGVGTFHFEK : 144
Zm PPH : VHAAQGFHVSDVDAALQGIPSMKAGEAERVMIQGLPE---GPDSSPISTGFWEWKPKLTVHYERSGMKNSKAPAVLFLPGFGVGTFHFEK : 149
Ot PPH : ------------------------------------------MTTTEGFYRWRGH-DAHYARCGATTATTH-VVFLPGFGVGTFHYEA :  44

                *       200       *       220       *       240       *       260       *
At PPH : QLTD--LGRDYRVWAIDFLGQGLSLPTEDPTTMTEETSSSEDKEPFWGFGDKTEPWADQLVFSLDLWRDQVQYFVEEVIGEPVYIAGNSL : 222
Vv PPH : QLKD--LGRDTRVWAVDFLGQGMSLPFEDPAFQSKKELDSERNDFSWGFGDETEPWANELVYSIDLWQDQVRYFIEQVIGEPVYIVGNSL : 265
Os PPH : QLKD--LGRDTKVWTMDFLGQGMSLPCEDPAFKSTSGELD--EDTYWGFGQELQPWAELVYSIDLWRDQVQHFIEEVIGEPVYIVGNSL : 230
Zm PPH : QLRD--LGRDHRVWTMDFLGQGMSLPGEDPAFSSIAS-----EDAFWGFGQDSQPWAELVYSVDLWQNQVQHFIEEVIREPVYIVGNSL : 232
Ot PPH : QLREGALGEDACAWALDFVGQGKSWPRG-----EEAIDG-------------------FAYSVDAWREQVEYFLREVVGREAYVCGNSL : 109

                280       *       300       *       320       *       340       *       360
At PPH : GGYVALYFAAIHP--HLVKGVTLLNATPFWGFFPNPVRSPKLARLFPWPGAFPLPERVKKITELVWQKISDPESIAEILKQVYTDHSINV : 310
Vv PPH : GGFVALYFAACNP--QLVKGVTLLNATPFWGFFPNPSRSPSLARIFPWAGTFPLPAFVRKLTEFVWQKISDPRSIGEVLKQVYADHSTKV : 353
Os PPH : GGFVSLYLAASCP--HLVKGVTLLNATPFWGFFPNPATSPRLSKIFPWAGTFPLPSFVRKLTETVWQKISDPRSIQGILKQVYADHSTNV : 318
Zm PPH : GGFVALYFAASSP--HLVKGVTLLNATPFWGFFPNPATSPRLSKIFPWAGTFPLPSFVRKITEAVWQKISDPKSIQDILKQVYADHSTNV : 320
Ot PPH : GGYVATYVAAAESSRDLVKGLILMNATPFWAFFPSDEESLGY-KLAPWRGSLPVPGWIRAPIKQYWESFRSRANVRGLLSLVYANAEAID : 198

                *       380       *       400       *       420       *       440       *
At PPH : DKVFSRIVEVTQHPAAAASFASIMLAPGGELSFSEALSRCKENNVQICLMYGREDPWVRPLWGKKIKKEIPNAPYYEISPAGHCPHDEVP : 400
Vv PPH : DKVFSRILETTQHPAAAASFASIMFAPQGQLSFSEALSRCQMSNVPICLMYGKEDPWVRPVWGLQVKKQLLEAPYYEISPAGHCPHDEVP : 443
Os PPH : DMVFSRIIETTQHPAAAASFASIMCAPKGQISFEEALSRCQRQGIPISLMYGREDPWVRPIWGIKVKQQVPESPYYEISPAGHCPHDEVP : 408
Zm PPH : DKVFSRIVEITQHPAAAASFASIMFAPRGQISFQEAISRCQDQGIPISLMYGREDPWIRPIWGLKVKQQVPEAPYYEISPAGHCPHDEVP : 410
Ot PPH : DRLIRDIIEPTENKNALSTFCSVVWSPKSAMSPDDMTERIRDSNIPVALVYGKEDPWVVPLWGQRLKKAIPRAHYYELSPVGHCPAHEAP : 288

                460       *       480       *       500       *       520       *
At PPH : EVVNYLMRGWIKHLESGGFEALPLLLDTEEDWEPSRIGRDIEFPRDGWKKAVNLWLYGSNYTYWRGVRESFRSSFIRVFGGKSA : 484
Vv PPH : EVVNYLLRGWIGNLESKGSVTLPLLD--DPENIQYGTTKDLEFVREGSKKSVRVHFYGSREFSLWNRIRSYVKSREFEALEINSR- : 524
Os PPH : EVINYLLRGWLKNVESEGSVAVPFLP--EPSYAENGVSREFLEFVRGGSKKSVHVRLFGSKISLWSQLRSLLKSNTWVISR----- : 486
Zm PPH : EVINYLLRGWLKNLESEGSVDLPFLP--ERSYAERGVSREFLEFVREGSRKSVSVRLYGTKISLWSQLSSFLNTRVPKSRIVLR- : 491
Ot PPH : ETVNSILSRYLQFCESTAEETQPPSG--SADGRAKLID-------------------GAPRNIFERIDAYRASRSPTM------ : 345
```

Figure 8. Phylogenetic Analysis and Sequence Alignment of PPH Homologs.

that *PPHs* are single-copy genes. Figure 8B shows an alignment of selected proteins from the PPH clade shown in Figure 8A. The proteins exhibited sequence identities between 38.6% (Ot PPH versus Os PPH) and 79.1% (Zm PPH versus Os PPH). Except for *Ostreococcus taurii*, all shown PPH proteins contained chloroplast transit peptides as predicted by ChloroP. An α/β hydrolase fold (InterPro IPR000120; Pfam PF00561) was present in all PPH proteins, but a screen in the InterPro database (http://www.ebi.ac.uk/Tools/InterProScan/) did not identify other known conserved motifs. However, a novel motif with the consensus sequence [AV]-x-[LIV]-x-G-N-S-[LIV]-G-G-[YF]-[LIV] (underlined in Figure 8B) was present, which we tentatively named the PPH motif and which was most similar to, but distinct from, the lipase GDSL motif of the PROSITE database (PS01098). The core sequence of the PPH motif (G-N-S-[LIV]-G-G) was also conserved in the proteins of clade II, but not clade III (see Supplemental Figure 7A online), indicating a possible related function of clade II proteins. To the best of our knowledge, none of the proteins in the tree have functionally been characterized. The active site of many hydrolytic enzymes is composed of a catalytic triad with a Ser residue that carries out the nucleophilic attack of the substrate (Dodson and Wlodawer, 1998). In analogy to PS01098 (see Supplemental Figure 7B online) and because PPH catalyzes the ester bond hydrolysis reaction from phein *a* to pheide *a* and phytol, the Ser residue of the PPH motif (marked with an arrowhead in Figure 8B) is likely the active-site Ser of PPHs. As shown above (Figures 2E and 7D), Ser-221 of *Arabidopsis* PPH was required for both in vitro PPH activity and *pph-1* complementation.

DISCUSSION

A Novel Candidate Protein for Chlorophyll Dephytylation in Senescent Leaves

The need for a phytol-cleaving reaction in chlorophyll breakdown is rationalized by the fact that the final breakdown products, NCCs, are water soluble and are located inside the vacuole (Matile et al., 1988). Phytol removal had been considered as an early reaction of the pathway, and mutants defective in either PAO (*pao1*) or red chlorophyll catabolite reductase (*acd2*) accumulate dephytylated pigments (Pružinská et al., 2003, 2007; Tanaka et al., 2003; Pružinská et al., 2005). Whereas red chlorophyll catabolites found in *acd2-2* during senescence are (partially) localized inside the vacuole (Pružinská et al., 2007), pheide *a* accumulating in *pao1* is retained in the plastid (S. Aubry and S. Hörtensteiner, unpublished results). These data indicate that phytol cleavage occurs rather early in the pathway and that the activity resides in the chloroplast. Nevertheless, the molecular identification of chlorophyllases questioned the exclusive location of dephytylation inside the plastid because several of the genes cloned so far indicated localization of the deduced proteins in the cytosol or vacuole (Takamiya et al., 2000). Experimental evidence for subcellular CLH localization using GFP fusions was ambiguous (Okazawa et al., 2006; Schenk et al., 2007), and in only one case, namely, *Citrus* Chlase1, has chloroplast localization been established immunologically (Harpaz-Saad et al., 2007; Azoulay Shemer et al., 2008). Nevertheless, the role of CLH in chlorophyll breakdown during leaf senescence remained elusive until our recent report, in which we demonstrated that CLHs are not essential for senescence-related chlorophyll breakdown in *Arabidopsis* (Schenk et al., 2007). We based our assumption on the analysis of *clh* single and double mutants, which were marginally affected in chlorophyll breakdown. In addition, CLH expression was not correlated with senescence (Liao et al., 2007; Schenk et al., 2007), and overexpression of CLHs in *Arabidopsis* did not accelerate leaf senescence (Benedetti and Arruda, 2002; Kariola et al., 2005). Here, we show that despite the presence of CLHs in *pph-1*, only small quantities of chlorophyll are converted to phytol-free NCCs. This supports our earlier finding of CLHs playing only a minor role in chlorophyll breakdown (Schenk et al., 2007), but the data presented here prompted us to suggest that PPH is a major chlorophyll-dephytylating enzyme during leaf senescence. By contrast, during fruit ripening of *Citrus limon*, levels of Chlase1 (a member of the CLH protein family) negatively correlated with chlorophyll amounts at the cellular level. Moreover, expression of the gene was increased by ethylene treatment, which also considerably accelerated chlorophyll breakdown (Azoulay Shemer et al., 2008). This implied that Chlase1 is involved in chlorophyll breakdown during *Citrus* fruit ripening (Azoulay Shemer et al., 2008), but further analysis is required to elucidate whether PPH might also have a role in fruits.

We identified PPH using a functional genomic approach, a powerful tool that has previously been used to identify the enzymes involved in chlorophyll breakdown at the molecular level (Pružinská et al., 2003). Deficiency of PPH resulted in a cosmetic stay-green phenotype (see below). In addition, *PPH* was highly coexpressed with and embedded within a network of genes involved in chlorophyll breakdown, namely, *PAO*, *NYC1*, and *SGR1*. The two other candidates obtained by this approach, namely, At1g54570 and At3g26840, were homologous to each other and had been shown in proteomic studies to localize to

Figure 8. (continued).

(A) Maximum likelihood phylogenetic tree of PPH and related proteins from plants, algae, and cyanobacteria. Branch support values obtained from 1,000 bootstraps are indicated when higher than 50%. Three clades (I, II, and III) are distinguished. For protein accession numbers, see Methods. At, *Arabidopsis thaliana*; Cr, *Chlamydomonas reinhardtii*; Nt, *Nicotiana tabacum*; Ol, *Ostreococcus lucimarinus*; Os, *Oryza sativa*; Ot, *Ostreococcus taurii*; Pp, *Physcomitrella patens*; Ps, *Picea sitchensis*; Pt, *Phaeodactylum tricornutum*; Sco, *Synechococcus* sp PCC 7002; Scy, *Synechocystis* sp PCC 6803; Vv, *Vitis vinifera*; Zm, *Zea mays*.

(B) Sequence alignment of PPH proteins from different species. Black shading with white letters, gray shading with white letters, and gray shading with black letters reflect 80, 60, and 40% sequence conservation, respectively, with Blosum62 similarity group enabled. A conserved domain (named the PPH domain) containing the proposed active-site Ser residue (arrowhead) is underlined.

plastoglobules (Vidi et al., 2006; Ytterberg et al., 2006). During leaf senescence, plastoglobules increase in size and number (Matile et al., 1999), and using electron tomography they were shown to form a continuum with the outer leaflet of the thylakoid membrane (Austin et al., 2006). Furthermore, plastoglobules contain large amounts of phytol and fatty acid phytyl esters (Gaude et al., 2007), and a salvage pathway of chlorophyll-derived phytol for tocopherol biosynthesis was recently established (Ischebeck et al., 2006). However, using single and double mutants, a direct role for At1g54570/At3g26840 in chlorophyll breakdown was not obvious.

PPH Is a Pheophytinase but Not a Chlorophyllase

The analysis of in vitro PPH activity after expression in *E. coli* yielded surprising results (Figure 7). The enzyme accepted phein as substrate, thereby both phein *a* and *b* were converted to the respective phytol-free pigments, pheide *a* and pheide *b*. By contrast, chlorophyll was not a substrate for the enzyme and did not inhibit pheophytinase activity in a competitive manner. In vitro–expressed CLH proteins, however, are much less specific and accept different porphyrinic substrates (see Supplemental Figure 5 online; Fiedor et al., 1992) but also unrelated hydrophobic esters, such as *p*-nitrophenyl decanoate (Arkus et al., 2005). The phein specificity of PPH was in agreement with the observation that *pph-1* accumulated substantial amounts of phein during leaf senescence. However, compared with the *pao1* mutant, which accumulates up to 150 μg pheide *a* g^{-1} leaf material (Pružinská et al., 2005), the amounts of phein found in *pph-1* (Figure 6D) were considerably smaller (~28 μg phein *a* g^{-1} leaf material). We speculated that PAO could act on phein *a*, yet phein *a* levels were not increased in a *pph-1 pao1* double mutant. Alternatively, an efficient (unknown) feedback mechanism might prevent further chlorophyll breakdown if the pathway is blocked. However, the fact that small quantities of NCCs accumulated in *pph-1* (Figure 6E) indicated some leakage, possibly the result of a limited participation of other hydrolases, such as CLHs.

Based on our results, we conclude that the order of the early reactions in chlorophyll breakdown during senescence is likely different than commonly assumed so far (Hörtensteiner, 2006). Thus, Mg release seems to precede phytol cleavage, resulting in the formation of intermediates in the following order: chlorophyll → phein → pheide. As a consequence, we propose a changed major route of chlorophyll metabolism, in which the reactions of chlorophyll biosynthesis and degradation are no longer linked through chlide as suggested earlier (Rüdiger, 2002) (Figure 9A). Instead, the anabolic and catabolic pathways are largely metabolically separated, but are connected through the chlorophyll cycle (Rüdiger, 2002). Thereby, the oxidative steps, catalyzed by chlorophyll *a* oxygenase (Tanaka et al., 1998), mainly occur at the level of phytol-free chlide, whereas *b* to *a* reduction, involving NYC1/NOL, mainly occurs at the level of chlorophyll.

Several published reports have described accumulation of various green intermediates of chlorophyll breakdown, including phein and pyropheophytin (Schoch et al., 1981; Schoch and Vielwerth, 1983; Amir-Shapira et al., 1987). However, dephytylated pigments, such as chlide, pheide, and pyropheophorbide, have been found as well (Amir-Shapira et al., 1987; Ziegler et al., 1988; Shimokawa et al., 1990; Shioi et al., 1991; Roca et al., 2004). Identification of Mg-free pheo intermediates is in agreement with the proposed route, but accumulation of chlide would argue against it. Chlide has been found both in fruits, such as *Citrus*, where chlorophyllase indeed seems to be involved in vivo (Azoulay Shemer et al., 2008), and in systems exhibiting rather high levels of in vitro chlorophyllase activity. Historically, chlorophyllase activity is determined in the presence of high concentrations of acetone or detergent (i.e., similar conditions as used for extraction of chlorophyll pigments from plant tissues). Thus, to determine in vivo quantities of chlide, care must be taken during pigment extraction to avoid artificial activation of chlorophyllases. As an example, in *Arabidopsis*, the fraction of chlide does not exceed 0.5% of total chlorophyll (Schenk et al., 2007), yet reports have been published claiming chlide fractions between 10 and 40% (Benedetti and Arruda, 2002; Kariola et al., 2005). Likewise, the occurrence of chlide in some stay-green mutants, such as *F. pratensis* Bf993 (Vicentini et al., 1995b), is correlated with advanced senescence, likely due to tissue rupture and subsequent nonphysiological chlorophyll hydrolysis (Aubry et al., 2008). In this work, only negligible amounts of chlide were found in the wild type or *pph-1* (Figure 6). In conclusion, we argue that the proposed route of chlorophyll breakdown during leaf senescence via phein instead of chlide does not conflict with data from the literature. However, the pathway involving PPH might be accompanied by additional, minor activities that convert some chlorophyll to chlide.

pph-1 Is a Nonfunctional Stay-Green Mutant Deficient in Chlorophyll Breakdown

The absence of PPH in *pph* mutants caused a stay-green phenotype, in which senescence parameters were uncoupled from chlorophyll breakdown. Thus, *pph* mutants can be classified as cosmetic, nonfunctional type C stay-greens (Thomas and Howarth, 2000). Despite the accumulation of phein *a* (see above), *pph* mutants did not exhibit a lesion-mimic phenotype. This is in contrast with *pao1* and *acd2*, which were shown to accumulate pheide *a* and red chlorophyll catabolites, respectively (Pružinská et al., 2005, 2007). Two hypotheses might explain this fact. First, the amount of phein accumulating in *pph* is not sufficient to cause cell death, or, second, phototoxicity of phein is prevented through its binding to LHCs. The latter is supported by the observation that, despite the loss of photosynthetic activity during senescence in *pph-1*, it is assumed that the mutant is able to dissipate light energy absorbed by the retained pigments. This is most likely achieved through the binding of chlorophyll to its apoproteins, but, as in the case of other nonfunctional stay-green mutants, the mechanism of energy quenching in *pph-1* remains unknown. Furthermore, even though senescence-regulated genes of chlorophyll breakdown, such as *PAO* and *SGR1*, are upregulated in *pph-1* (Figure 3), as they are in the wild type, chlorophyll breakdown is prevented. It is likely that the porphyrin pigments remain attached to their apoproteins as long as they carry the phytol moiety and are thus not accessible to further downstream catabolic enzymes. This view is supported by the fact that in *pph-1* or other stay-green mutants, such as

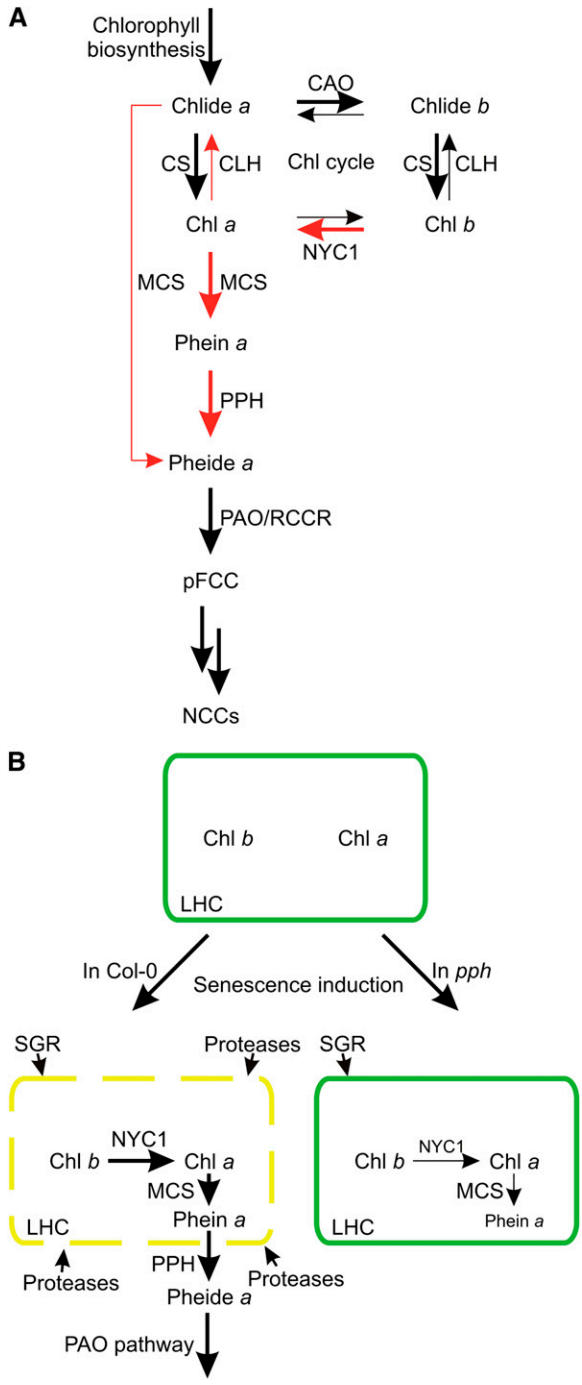

Figure 9. Tentative Models for Chlorophyll Metabolism and for Chlorophyll-Apoprotein Degradation.

(A) Schematic drawing of chlorophyll biosynthesis and degradation, integrating the findings of this work. In this model, anabolic and catabolic steps do not have overlapping activities but are interconnected through the chlorophyll cycle. Thickness of arrows within the cycle reflects relative activities of respective enzymes as suggested by Rüdiger (2002). CLHs might marginally contribute to chlorophyll degradation (thin red arrows), but the bulk of chlorophyll seems to be catabolized via phein *a* and PPH (thick red arrows).

nye1 or *nyc1* (Kusaba et al., 2007; Ren et al., 2007), no increase in free chlorophyll has been observed. In this respect, it is important to note that *pph-1* is particularly defective in chlorophyll *b* degradation, and it thus has a phenotype that greatly resembles that of *nyc1*. However, *NYC1* and *NOL* expression were not altered in *pph-1* compared with the wild type, and further analysis is required to elucidate whether chlorophyll *b* reductase activity is affected in *pph-1*. *pph-1* accumulated phein *a* but not phein *b*, indicating that the *b* to *a* conversion occurs before phytol hydrolysis. A tentative model of reactions required for chlorophyll-apoprotein degradation can be drawn, integrating published data and the results obtained in this work (Figure 9B). In this model, the concerted activity of (at least) three proteins (i.e., SGR, NYC1, and PPH) is required for the initiation of LHC protein degradation. The stromal localization of PPH implies that phein would be released from the complex before hydrolysis; however, PPH more likely transiently associates with components of the thylakoid membrane during catalysis. Similar interactions have been shown between envelope-bound PAO and stromal red chlorophyll catabolite reductase (Pružinská et al., 2007) and between LHC subunits and stroma-localized SGR (Park et al., 2007). LHCs are largely retained in *pph-1*; thus, it seems reasonable to assume that dephytylation (through PPH) is required for pigment release from the complexes as a prerequisite for the subsequent proteolytic degradation of the apoproteins. Alternatively, stabilization of LHC in *pph-1* could be achieved by preventing further chlorophyll *b* to chlorophyll *a* conversion as a consequence of phein *a* retention in the mutant.

PPH Is a Member of a Novel Subclass of α/β Hydrolases

From the distribution of PPH and PPH-like proteins in a phylogenetic tree (Figure 8), it can be hypothesized that they are all derived from an ancestral bacterial esterase gene that was duplicated twice. After endosymbiosis, one gene copy was recruited as PPH. This view is supported by the fact that each of the eukaryotic genomes analyzed contained a single copy of PPH, which was significantly distinct from the two other clades of the tree. In addition, the PPH clade did not contain a bacterial ortholog, indicating that PPH is absent from cyanobacteria. This is in agreement with recent labeling studies for chlorophyll

(B) Tentative model for the degradation of LHC-chlorophyll complexes during senescence in Col-0 and *pph-1*. Upon senescence induction in the wild type, SGR, NYC1, and PPH are activated. Acting independently or in concert, these induced proteins cause structural changes and/or partial destabilization of the LHC-chlorophyll complexes, at least in part through chlorophyll *b* to chlorophyll *a* conversion catalyzed by NYC1. By contrast, the function of SGR in this process is not resolved yet. These changes allow proteases to access and degrade the apoproteins. In the absence of PPH in *pph* mutants, LHC complexes are stabilized and not accessible for proteases, possibly because of the retention of phytylated pigments within the complexes. Alternatively, LHCs could be stabilized by preventing/slowing down further chlorophyll *b* to *a* conversion as a consequence of phein *a* accumulation.

CAO, chlide *a* oxygenase; Chl, chlorophyll. CS, chl synthase; MCS, metal-chelating substance; RCCR, red chlorophyll catabolite reductase.

synthesis and degradation in *Synechocystis* sp PCC 6803, demonstrating that a continuous chlorophyll dephytylation/chlide rephytylation cycle operates in cyanobacteria (Vavilin and Vermaas, 2007). However, *Synechocystis* sp PCC 6803 does not contain a gene with significant homology to CLHs; therefore, the nature of the phytol cleaving activity remains unknown (Vavilin and Vermaas, 2007). The presence of PPH proteins in evolutionary divergent plant species substantiates the likelihood of a common, important function for these proteins.

The primary amino acid sequences of PPH proteins exhibited several domains that are highly conserved between the members. Among these was a motif (named the PPH domain) with a conserved Ser residue, which, based on homology to nearly 500 hydrolases from bacteria to humans, most likely represents the active-site residue (see Supplemental Figure 7C online). Site-directed mutagenesis of the Ser residue seemed to confirm this, although we cannot exclude that the mutation might have impaired proper PPH folding, thereby causing the observed loss of function. The PPH domain was most similar to, but distinct from, a lipase domain (PROSITE PS01098) containing the core sequence G-D-S-[LIVM]. In PPHs, Asp is replaced by an invariant Asn residue, which could be involved in defining substrate specificity. By contrast, CLH proteins contain another PROSITE domain (PS00120) with the core consensus G-[HYVW]-S-x-G (see Supplemental Figure 7B online). The active site of many α/β hydrolases, including proteases and lipases, is composed of a catalytic triad that, in addition to the active Ser residue, involves a His and Asp residue (Dodson and Wlodawer, 1998). Several of these residues are conserved within PPH proteins; which of them are essential for PPH activity remains to be elucidated by site-directed mutagenesis.

In conclusion, we have identified an esterase, named PPH, that is involved in chlorophyll breakdown during leaf senescence. Our data demonstrate that the absence of PPH causes indefinite retention of greenness. We furthermore provide in vitro and in vivo evidence that PPH specifically cleaves the phytol ester of phein, but not chlorophyll. We propose that PPH is the major dephytylating activity in chlorophyll breakdown and is active downstream of chlorophyll *b* reductase (NYC1). Hence, the sequence of early reactions in chlorophyll breakdown has to be reconsidered and very likely proceeds in the following order: chlorophyll *b* → chlorophyll *a* → phein *a* → pheide *a*. Further analysis will be required to analyze whether PPH might also be involved in other instances of chlorophyll metabolism, such as chlorophyll turnover at the steady state level or during fruit ripening.

METHODS

Plant Material and Senescence Induction

Arabidopsis thaliana ecotype Col-0 was used as the wild type. T-DNA insertion lines were from the following collections: SALK (Alonso et al., 2003): *at5g13800-1* (*pph-1*), SALK_000095; *at1g54570-1*, SALK_034549; *at3g26840-1*, SALK_071769; JIC SM lines (Tissier et al., 1999): *pph-2*, SM_3_15198, and GABI lines (Rosso et al., 2003): *pph-3*, GABI_453A08. SALK and SM lines were obtained from the European Arabidopsis Stock Center, Nottingham, UK. The GABI line was obtained from GABI Kat, MPI for Plant Breeding Research, Cologne, Germany. Homozygous plants were identified by PCR using T-DNA-, transposon-, and gene-specific primers as listed in Supplemental Table 1 online. Likewise, homozygous *at1g54570-1 at3g26840-1* and *pph-1 pao1* double mutants were identified by PCR. Plants were grown on soil in long-day conditions in a greenhouse with fluence rates of 100 to 200 μmol photons m^{-2} s^{-1} at 22°C. For senescence induction, detached leaves of 3- to 4-week-old plants were incubated on wet filter paper for up to 7 d in the dark. Alternatively, individual attached leaves were covered with aluminum foil.

Biocomputational Methods and Phylogenetic Analysis

We screened the TAIR8 protein database (http://www.Arabidopsis.org) for hits containing the phrase "alpha/beta." Using the BULK PROTEIN ANALYSIS tool, a subset of 462 proteins was analyzed for proteins containing a putative plastid-targeting sequence. Screening for known protein function was done with the GENE ONTOLOGY ANNOTATION tool.

Homologs of PPH were identified by BLASTP searches (Altschul et al., 1997) with databases of the National Center for Biotechnology Information (http://www.ncbi.nlm.nih.gov) and the Joint Genome Institute (http://www.jgi.doe.gov). For phylogenetic analysis, multiple sequence alignment of PPH amino acid sequences was generated with PROMALS3D (Pei et al., 2008) using default settings. The alignment was curated using Gblocks 0.91b (Talavera and Castresana, 2007) with the following parameters: 15, minimum number of sequences for conserved and flanking positions: 120, maximum number of continuous nonconserved positions; 2, minimum length of a block; all, gap positions. The maximum likelihood tree was obtained with PhyML 3.0 (http://www.atgc-montpellier.fr/phyml; Guindon and Gascuel, 2003) using the LG+I+Γ model (Le and Gascuel, 2008) with four substitution rate categories and estimated gamma shape parameter and proportion of invariant sites. Default settings were used for other parameters. Branch support values are based on 1000 nonparametric bootstrap replicates.

For Figure 8B and Supplemental Figure 7 online, sequences were aligned using the programs DIALIGN (Morgenstern, 2004), GENEDOC (http://www.psc.edu/biomed/genedoc), and WebLogo (http://weblogo.threeplusone.com).

pph-1 Complementation

A full-length cDNA sequence of *PPH* was obtained from the RIKEN resource (Seki et al., 2002). In a two-step PCR amplification using Pfu polymerase (Promega) and the primers listed in Supplemental Table 1 online, Gateway BP recombination sites were added to the *PPH* cDNA. *PPH* was cloned behind the 35S promoter of the destination vector pMDC32 (Curtis and Grossniklaus, 2003) using Gateway technology (Invitrogen). Likewise, a *PPH* $S_{221}A$ missense mutation was produced in pMDC32. Two overlapping PCR fragments containing the mutation were produced by PCR using Pfu polymerase, attB1, and gene-specific primers as listed in Supplemental Table 1 online. In a second PCR reaction, the fragments were combined to yield PPH_{S221A} that, after verification by sequencing, was introduced behind the 35S promoter of pMDC32 (*35S:*PPH_{S221A}) using Gateway technology. *pph-1* was transformed with the flower dip method (Clough and Bent, 1998). Transformants were selected on hygromycin, and homozygous T2 plants were used for further analysis.

GFP Fusion Protein Analysis

PPH cDNA was PCR amplified using the primers listed in Supplemental Table 1 online and cloned into pMDC84 (Curtis and Grossniklaus, 2003) by Gateway technology, thereby producing an N-terminal fusion of PPH

with GFP (PPH-GFP). *Arabidopsis* mesophyll protoplasts were isolated from 6-week-old short-day-grown plants according to published procedures (Endler et al., 2006). Cell numbers were quantified with a Neubauer chamber and adjusted to a density of 2×10^6 protoplasts mL^{-1}. Protoplasts were transformed by 20% polyethylene glycol transformation according to published procedures (Meyer et al., 2006). Transformed cells were incubated for 48 h in the dark at room temperature before laser scanning confocal microscopic analysis (DM IRE2; Leica Microsystems). GFP fluorescence was imaged at an excitation wavelength of 488 nm, and the emission signal was recovered between 495 and 530 nm. TIC110-GFP expressed from pCL60-TIC110-GFP (Schenk et al., 2007) was used as a control for plastid envelope localization.

Protein Import Experiments

[^{35}S]-Met–labeled PPH was synthesized from *Arabidopsis* full-length *PPH* cloned in pBluescript with the TNT T7 Quick Coupled Transcription/Translation System (Promega). Intact chloroplasts of 4-week-old in vitro–grown *Arabidopsis* plants (ecotype Col-2) were isolated as published (Kubis et al., 2008) with the following modifications. The chloroplast isolation buffer was composed of 50 mM HEPES-KOH, pH 7.5, 2 mM EDTA, 1 mM $MnCl_2$, 1 mM $MgCl_2$, 330 mM sorbitol, 100 mM Na-ascorbate, 0.25% BSA, and 0.05% protease inhibitor cocktail (Sigma-Aldrich). Chloroplasts were purified on a 40/85% step gradient of Percoll (GE Healthcare) in 300 mM sorbitol, 20 mM Tricine-KOH, pH 8.5, 5 mM $MgCl_2$, and 2.5 mM EDTA. PPH import assays were performed as published (Fitzpatrick and Keegstra, 2001). For each import reaction, chloroplasts corresponding to 15 μg of chlorophyll and 6.5 μL of in vitro–translated PPH preprotein were used. Lysis of chloroplasts, separation of stroma from membranes, and alkaline membrane treatment were done as described (Smith et al., 2002). All samples were resolved by SDS-PAGE and visualized using a phosphor imager (Bio-Rad).

RNA Isolation and RT-PCR

RNA was isolated using the Plant RNeasy kit (Qiagen). After DNA digestion with RQ1 DNase (Promega), first-strand cDNA was synthesized using the RETROscript kit (Ambion). PCR was performed with a non-saturating number of amplification cycles as shown in the figures using gene-specific primers as listed in Supplemental Table 1 online.

Analysis of Chlorophyll and Chlorophyll Catabolites

For spectrophotometric determination of chlorophyll concentrations (Strain et al., 1971), chlorophyll was extracted from leaf tissue by homogenization in liquid nitrogen and subsequent threefold extraction into 80% (v/v) acetone containing 1 μM KOH. After centrifugation (2 min; 16,000*g*), supernatants were combined and used for analysis.

For HPLC analysis of green chlorophyll catabolites (chlorophyll, chlide, pheide, and phein), liquid nitrogen-homogenized tissue was extracted in 10% (v/v) 0.2 M Tris-HCl, pH 8, in acetone, cooled to –20°C (20 mL g^{-1} fresh weight), and incubated at –20°C for 2 h in the dark. After removal of insoluble material by centrifugation, supernatants were analyzed by reverse-phase HPLC as described (Pružinská et al., 2005). Pigments were identified by their absorption spectra, peak ratios, and comigration with authentic standards (Roca et al., 2004). For quantification, chlorophyll solutions of defined concentrations were analyzed by HPLC, and peak areas at A_{665} referred to the injected quantities. Likewise, pheo pigments obtained after acidification of chlorophyll solutions (see below) were quantified spectrophotometrically (Porra, 1991) and used to calibrate HPLC peak areas.

NCCs were extracted from leaf tissue and analyzed as described (Pružinská et al., 2005).

Chlorophyll Fluorescence and CO_2 Assimilation Rate

Senescence was induced by darkening attached leaves with aluminum foil. Maximum quantum yield of PSII (F_v/F_m) was measured with a portable photosynthesis system LI-COR 6400 (Li-Cor). Rates of CO_2 assimilation were determined at a flux density of 0 to 1000 μmol m^{-2} s^{-1} and a CO_2 concentration of 380 μmol mol^{-1}.

Analysis of Recombinant PPH

For heterologous expression of PPH in *Escherichia coli*, a truncated fragment of *PPH* cDNA, lacking the 46 5′-terminal amino acids encoding the predicted chloroplast transit peptide, was produced by PCR using Pfu polymerase and the primers listed in Supplemental Table 1 online. After restriction digest with *Bam*HI/*Sal*I, the fragment was cloned into pMAL-c2 (New England Biolabs), producing an MBP-truncated PPH (ΔPPH) fusion (MBP-ΔPPH). Likewise, a S_{221}A missense mutation was introduced into ΔPPH by PCR as described above and cloned into pMAL-c2 (MBP-ΔPPH_{S221A}). After verification of constructs by sequencing, recombinant proteins were allowed to accumulate after chemical induction of gene expression for 3 h as described (Wüthrich et al., 2000). Cells were lysed by lysozyme treatment and sonication as described (Wüthrich et al., 2000) using 0.1 M MOPS-KOH, pH 7.0, as buffer. Crude cell extracts were supplemented with 10% (v/v) glycerol and either directly used for assays or frozen in liquid nitrogen, which did not affect enzyme activity. For MBP fusion protein cleavage, *E. coli* extracts were treated for 24 h with factor XA (50 mg g^{-1} protein) according to the manufacturer's protocol (New England Biolabs). Recombinant *Citrus* Chlase1 was expressed as a thioredoxin fusion protein as described (Jakob-Wilk et al., 1999). Crude Chlase1 extracts were produced as above.

The assays (total volume 200 μL) consisted of 10 μL crude cell extracts (corresponding to 0.36 mL of original cell culture at $OD_{600} = 1.5$) and 20 μL of pigment substrates dissolved in acetone (final concentration of pigment substrates, 29 μM; final acetone concentration, 10%). After incubation at 25°C for various time periods as indicated in the figures, the reaction was stopped by the addition of acetone to a final concentration of 66%. After centrifugation (2 min at 18,000*g*), samples were analyzed by HPLC as described above. Chlorophyll used as substrate was isolated from coffee (*Coffea arabica*) leaves as described (Vicentini et al., 1995a) and quantified photometrically (Strain et al., 1971). For the production of phein, the chlorophyll solution was acidified by the addition of HCl to a final concentration of 20 mM. After 2 min, 20 mM NaOH (final concentration) was added to neutralize the solution, which was then employed as substrate in the assays.

Extraction and Analysis of Photosystem Subcomplexes

Chloroplast membranes were isolated according to established procedures (Oh et al., 2003). Membranes were subsequently solubilized on ice for 30 min with 0.8% (w/v) dodecylmaltoside in 1× PBS. After centrifugation (5 min, 15,000*g*, 4°C), complexes were separated on a linear gradient of 1.0 to 0.1 M sucrose in 50 mM Tris-HCl, pH 8 (0.05%, w/v) dodecylmaltoside. After centrifugation at 4°C (197,000*g* for 16 h), 0.5 mL fractions were withdrawn with a gradient former (AutoDensiFlow II; Buchler) and analyzed by immunoblotting (see below).

Protein Extraction and Immunoblot Analysis

Total leaf protein and soluble and membrane fractions were prepared essentially as described (Pružinská et al., 2003; Schenk et al., 2007). SDS-PAGE and subsequent immunoblot analysis were performed as described (Pružinská et al., 2007). The following antibodies were used: monoclonal antibodies against PAO (1:500; Gray et al., 2004) and polyclonal antibodies against LHCa1, LHCa2, LHCb1, LHCb2, PsbA

(1:2000; AgriSera), PsaA (1:5000; J.D. Rochaix, Geneva, Switzerland), and Rubisco large subunit (1:2000; S. Gepstein, Haifa, Israel).

Transmission Electron Microscopy

Leaf segments (2 × 20 mm) were fixed at room temperature in 2.5% (v/v) glutaraldehyde and 1% (w/v) formaldehyde (freshly prepared from paraformaldehyde) in 0.1 M sodium cacodylate buffer, pH 7.3. After washing in buffer, the samples were postfixed in buffered 1% osmium tetroxide, washed, dehydrated in a graded series of ethanol, and embedded in LR white resin. The resin was polymerized at 60°C. Ultrathin sections were cut with a diamond knife in an Ultracut UCT ultramicrotome (Leica). The sections were stained with saturated uranyl acetate in water and lead citrate (Reynolds, 1963) and observed using a Philips CM10 transmission electron microscope.

Accession Numbers

Protein sequences used in this work are as follows. GenBank identification numbers: *Arabidopsis thaliana* (At): At PPH, 15240707 (At5g13800); At4g36530, 15234433; At5g19850, 26450541; SGR1, 18416035 (At4g22920); PAO, 15230543 (At3g44880); NYC1, 18413962 (At4g13250); NOL, 18414726 (At5g04900); CLH1, 18394772 (At1g19670); CLH2, 15240020 (At5g43860); *Chlamydomonas reinhardtii* (Cr): Cr PPH, 159490010; Cr XP1701, 159486857; Cr XP1698, 159480594; *Citrus sinensis* (Cs): Chlase1, 7328567; *Nicotiana tabacum* (Nt): Nt PPH, 156763846; *Ostreococcus lucimarinus* (Ol): Ol PPH, 145340970; Ol XP1422, 145355583; *Oryza sativa* (Os): Os PPH, 115467988 (Os06g0354700); Os EAZ404, 125600825; Os EAZ243, 125583397; *Ostreococcus taurii* (Ot): Ot PPH, 116000661; Ot CAL579, 116055845; *Physcomitrella patens* (Pp): Pp PPH, 168018382; Pp XP1785, 168067769; Pp XP1762, 168019983; *Picea sitchensis* (Ps): Ps ABK247, 116788178; *Synechococcus* sp PCC 7002 (Sco): Sco YP1733, 170076657; Sco YP1734, 170077791; Sco YP1735, 170078876; *Synechocystis* sp PCC 6803 (Scy): Scy slr1917, 16329733; Scy slr1235, 16330114; *Vitis vinifera* (Vv): Vv PPH, 157350650; Vv CAO228, 157348115; *Zea mays* (Zm): Zm PPH, 194706646; Zm ACF844, 194,700,822. *Phaeodactylum tricornutum* (Pt) protein IDs are from the Joint Genome Initiative (http://jgi.doe.gov): Pt PPH, 41648; Pt 4967, 4967.

Supplemental Data

The following materials are available in the online version of this article.

Supplemental Figure 1. Natural Senescence of Col-0 and *pph-1*.

Supplemental Figure 2. Changes in Net Photosynthesis during Senescence in *pph-1*.

Supplemental Figure 3. Immunoblot Analysis of Photosynthetic Complexes after Sucrose Density Gradient Centrifugation.

Supplemental Figure 4. Accumulation of Chlorophyll *a* Derivatives in *pph-1*.

Supplemental Figure 5. Activity Determination of Recombinant *Citrus* Chlorophyllase.

Supplemental Figure 6. Activity Determination of Recombinant PPH.

Supplemental Figure 7. Sequence Alignment of the Active-Site Domain of PPH and PPH-Like Proteins.

Supplemental Table 1. Primers Used in This Work.

Supplemental Data Set 1. Sequences Used to Generate the Phylogenetic Tree Presented in Figure 8A.

ACKNOWLEDGMENTS

For the supply of antibodies, we thank John Gray (University of Toledo) (PAO), Shimon Gepstein (Israel Institute of Technology) (Rubisco large subunit), and Jean-David Rochaix (University of Geneva, Switzerland) (PsaA). Smadar Harpaz-Saad and Yoram Eyal (Volcani Center, Israel) kindly provided a bacterial strain expressing recombinant *Citrus* chlorophyllase. We thank Maria Mulisch (University of Kiel, Germany) for electron microscopy analysis. Support by grants from the Swiss National Science Foundation (3100A0-117940), to S.H., the National Center of Competence in Research Plant Survival, the research program of the Swiss National Science Foundation to S.H. and F.K., and the Global Research Laboratory program of the Ministry of Science and Technology of Korea to B.B. is acknowledged.

Received October 30, 2008; revised February 12, 2009; accepted March 8, 2009; published March 20, 2009.

REFERENCES

Alonso, J.M., et al. (2003). Genome-wide insertional mutagenesis of *Arabidopsis thaliana.* Science **301:** 653–657.

Altschul, S.F., Madden, T.L., Schaffer, A.A., Zhang, J.H., Zhang, Z., Miller, W., and Lipman, D.J. (1997). Gapped BLAST and PSI-BLAST: A new generation of protein database search programs. Nucleic Acids Res. **25:** 3389–3402.

Amir-Shapira, D., Goldschmidt, E.E., and Altman, A. (1987). Chlorophyll catabolism in senescing plant tissues: *In vivo* breakdown intermediates suggest different degradative pathways for *Citrus* fruit and parsley leaves. Proc. Natl. Acad. Sci. USA **84:** 1901–1905.

Arkus, K.A.J., Cahoon, E.B., and Jez, J.M. (2005). Mechanistic analysis of wheat chlorophyllase. Arch. Biochem. Biophys. **438:** 146–155.

Armstead, I., et al. (2006). From crop to model to crop: identifying the genetic basis of the staygreen mutation in the *Lolium*/*Festuca* forage and amenity grasses. New Phytol. **172:** 592–597.

Armstead, I., et al. (2007). Cross-species identification of Mendel's *I* locus. Science **315:** 73.

Aubry, S., Mani, J., and Hörtensteiner, S. (2008). Stay-green protein, defective in Mendel's green cotyledon mutant, acts independent and upstream of pheophorbide *a* oxygenase in the chlorophyll catabolic pathway. Plant Mol. Biol. **67:** 243–256.

Austin, J.R., Frost, E., Vidi, P.A., Kessler, F., and Staehelin, L.A. (2006). Plastoglobules are lipoprotein subcompartments of the chloroplast that are permanently coupled to thylakoid membranes and contain biosynthetic enzymes. Plant Cell **18:** 1693–1703.

Azoulay Shemer, T., Harpaz-Saad, S., Belausov, E., Lovat, N., Krokhin, O., Spicer, V., Standing, K.G., Goldschmidt, E.E., and Eyal, Y. (2008). *Citrus* chlorophyllase dynamics at ethylene-induced fruit color-break; a study of chlorophyllase expression, post-translational processing kinetics and *in-situ* intracellular localization. Plant Physiol. **148:** 108–118.

Barry, C.S., McQuinn, R.P., Chung, M.Y., Besuden, A., and Giovannoni, J.J. (2008). Amino acid substitutions in homologs of the STAY-GREEN protein are responsible for the *green-flesh* and *chlorophyll retainer* mutations of tomato and pepper. Plant Physiol. **147:** 179–187.

Benedetti, C.E., and Arruda, P. (2002). Altering the expression of the chlorophyllase gene *ATHCOR1* in transgenic Arabidopsis caused changes in the chlorophyll-to-chlorophyllide ratio. Plant Physiol. **128:** 1255–1263.

Borovsky, Y., and Paran, I. (2008). Chlorophyll breakdown during pepper fruit ripening in the *chlorophyll retainer* mutation is impaired at

the homolog of the senescence-inducible stay-green gene. Theor. Appl. Genet. **117:** 235–240.

Clough, S.J., and Bent, A.F. (1998). Floral dip: A simplified method for *Agrobacterium*-mediated transformation of *Arabidopsis thaliana.* Plant J. **16:** 735–743.

Curtis, M.D., and Grossniklaus, U. (2003). A gateway cloning vector set for high-throughput functional analysis of genes in planta. Plant Physiol. **133:** 462–469.

Dodson, G., and Wlodawer, A. (1998). Catalytic triads and their relatives. Trends Biochem. Sci. **23:** 347–352.

Emanuelsson, O., Nielsen, H., and Von Heijne, G. (1999). ChloroP, a neural network-based method for predicting chloroplast transit peptides and their cleavage sites. Protein Sci. **8:** 978–984.

Endler, A., Meyer, S., Schelbert, S., Schneider, T., Weschke, W., Peters, S.W., Keller, F., Baginsky, S., Martinoia, E., and Schmidt, U.G. (2006). Identification of a vacuolar sucrose transporter in barley and Arabidopsis mesophyll cells by a tonoplast proteomic approach. Plant Physiol. **141:** 196–207.

Fiedor, L., Rosenbach-Belkin, V., and Scherz, A. (1992). The stereospecific interaction between chlorophylls and chlorophyllase - Possible implication for chlorophyll biosynthesis and degradation. J. Biol. Chem. **267:** 22043–22047.

Fitzpatrick, L.M., and Keegstra, K. (2001). A method for isolating a high yield of Arabidopsis chloroplasts capable of efficient import of precursor proteins. Plant J. **27:** 59–65.

Fojan, P., Jonson, P.H., Petersen, M.T.N., and Petersen, S.B. (2000). What distinguishes an esterase from a lipase: A novel structural approach. Biochimie **82:** 1033–1041.

Gaude, N., Brehelin, C., Tischendorf, G., Kessler, F., and Dörmann, P. (2007). Nitrogen deficiency in Arabidopsis affects galactolipid composition and gene expression and results in accumulation of fatty acid phytyl esters. Plant J. **49:** 729–739.

Gray, J., Wardzala, E., Yang, M., Reinbothe, S., Haller, S., and Pauli, F. (2004). A small family of LLS1-related non-heme oxygenases in plants with an origin amongst oxygenic photosynthesizers. Plant Mol. Biol. **54:** 39–54.

Guindon, S., and Gascuel, O. (2003). A simple, fast, and accurate algorithm to estimate large phylogenies by maximum likelihood. Syst. Biol. **52:** 696–704.

Harpaz-Saad, S., Azoulay, T., Arazi, T., Ben-Yaakov, E., Mett, A., Shiboleth, Y.M., Hörtensteiner, S., Gidoni, D., Gal-On, A., Goldschmidt, E.E., and Eyal, Y. (2007). Chlorophyllase is a rate-limiting enzyme in chlorophyll catabolism and is posttranslationally regulated. Plant Cell **19:** 1007–1022.

Hinder, B., Schellenberg, M., Rodoni, S., Ginsburg, S., Vogt, E., Martinoia, E., Matile, P., and Hörtensteiner, S. (1996). How plants dispose of chlorophyll catabolites. Directly energized uptake of tetrapyrrolic breakdown products into isolated vacuoles. J. Biol. Chem. **271:** 27233–27236.

Horn, R., and Paulsen, H. (2004). Early steps in the assembly of light-harvesting chlorophyll *a*/*b* complex - Time-resolved fluorescence measurements. J. Biol. Chem. **279:** 44400–44406.

Hörtensteiner, S. (2006). Chlorophyll degradation during senescence. Annu. Rev. Plant Biol. **57:** 55–77.

Hörtensteiner, S., Vicentini, F., and Matile, P. (1995). Chlorophyll breakdown in senescent cotyledons of rape, *Brassica napus* L.: Enzymatic cleavage of phaeophorbide *a in vitro.* New Phytol. **129:** 237–246.

Hörtensteiner, S., Wüthrich, K.L., Matile, P., Ongania, K.-H., and Kräutler, B. (1998). The key step in chlorophyll breakdown in higher plants. Cleavage of pheophorbide *a* macrocycle by a monooxygenase. J. Biol. Chem. **273:** 15335–15339.

Ischebeck, T., Zbierzak, A.M., Kanwischer, M., and Dörmann, P. (2006). A salvage pathway for phytol metabolism in *Arabidopsis.* J. Biol. Chem. **281:** 2470–2477.

Jakob-Wilk, D., Holland, D., Goldschmidt, E.E., Riov, J., and Eyal, Y. (1999). Chlorophyll breakdown by chlorophyllase: Isolation and functional expression of the *Chlase1* gene from ethylene-treated *Citrus* fruit and its regulation during development. Plant J. **20:** 653–661.

Jiang, H., Li, M., Liang, N., Yan, H., Wei, Y., Xu, X., Liu, J., Xu, Z., Chen, F., and Wu, G. (2007). Molecular cloning and function analysis of the *stay green* gene in rice. Plant J. **52:** 197–209.

Kariola, T., Brader, G., Li, J., and Palva, E.T. (2005). Chlorophyllase 1, a damage control enzyme, affects the balance between defense pathways in plants. Plant Cell **17:** 282–294.

Kräutler, B. (2003). Chlorophyll breakdown and chlorophyll catabolites. In The Porphyrin Handbook, vol. 13, K.M. Kadish, K.M. Smith, and R. Guilard, eds (Oxford, UK: Elsevier Science), pp. 183–209.

Kräutler, B., and Hörtensteiner, S. (2006). Chlorophyll catabolites and the biochemistry of chlorophyll breakdown. In Chlorophylls and Bacteriochlorophylls: Biochemistry, Biophysics, Functions and Applications, B. Grimm, R. Porra, W. Rüdiger, and H. Scheer, eds (Dordrecht, The Netherlands: Springer), pp. 237–260.

Kräutler, B., Jaun, B., Bortlik, K.-H., Schellenberg, M., and Matile, P. (1991). On the enigma of chlorophyll degradation: the constitution of a secoporphinoid catabolite. Angew. Chem. Int. Ed. Engl. **30:** 1315–1318.

Kreuz, K., Tommasini, R., and Martinoia, E. (1996). Old enzymes for a new job. Herbicide detoxification in plants. Plant Physiol. **111:** 349–353.

Kubis, S.E., Lilley, K.S., and Jarvis, P. (2008). Isolation and preparation of chloroplasts from *Arabidopsis thaliana* plants. Methods Mol. Biol. **425:** 171–186.

Kusaba, M., Ito, H., Morita, R., Iida, S., Sato, Y., Fujimoto, M., Kawasaki, S., Tanaka, R., Hirochika, H., Nishimura, M., and Tanaka, A. (2007). Rice NON-YELLOW COLORING1 is involved in light-harvesting complex II and grana degradation during leaf senescence. Plant Cell **19:** 1362–1375.

Le, S.Q., and Gascuel, O. (2008). An improved general amino acid replacement matrix. Mol. Biol. Evol. **25:** 1307–1320.

Liao, Y., An, K., Zhou, X., Chen, W.-J., and Kuai, B.-K. (2007). *AtCLH2*, a typical but possibly distinctive chlorophyllase gene in *Arabidopsis.* J. Integr. Plant Biol. **49:** 531–539.

Matile, P., Ginsburg, S., Schellenberg, M., and Thomas, H. (1988). Catabolites of chlorophyll in senescing barley leaves are localized in the vacuoles of mesophyll cells. Proc. Natl. Acad. Sci. USA **85:** 9529–9532.

Matile, P., Hörtensteiner, S., and Thomas, H. (1999). Chlorophyll degradation. Annu. Rev. Plant Physiol. Plant Mol. Biol. **50:** 67–95.

Matile, P., Schellenberg, M., and Peisker, C. (1992). Production and release of a chlorophyll catabolite in isolated senescent chloroplasts. Planta **187:** 230–235.

Meyer, A., Eskandari, S., Grallath, S., and Rentsch, D. (2006). AtGAT1, a high affinity transporter for γ-aminobutyric acid in *Arabidopsis thaliana.* J. Biol. Chem. **281:** 7197–7204.

Morgenstern, B. (2004). DIALIGN: Multiple DNA and protein sequence alignment at BiBiServ. Nucleic Acids Res. **32:** W33–W36.

Mühlecker, W., Ongania, K.-H., Kräutler, B., Matile, P., and Hörtensteiner, S. (1997). Tracking down chlorophyll breakdown in plants: Elucidation of the constitution of a 'fluorescent' chlorophyll catabolite. Angew. Chem. Int. Ed. Engl. **36:** 401–404.

Müller, T., Moser, S., Ongania, K.-H., Pružinská, A., Hörtensteiner, S., and Kräutler, B. (2006). A divergent path of chlorophyll breakdown in the model plant *Arabidopsis thaliana.* ChemBioChem **7:** 40–42.

Oberhuber, M., Berghold, J., Breuker, K., Hörtensteiner, S., and

Kräutler, B. (2003). Breakdown of chlorophyll: A nonenzymatic reaction accounts for the formation of the colorless "nonfluorescent" chlorophyll catabolites. Proc. Natl. Acad. Sci. USA **100:** 6910–6915.

Oh, M.H., Moon, Y.H., and Lee, C.H. (2003). Increased stability of LHCII by aggregate formation during dark-induced leaf senescence in the *Arabidopsis* mutant, *ore10.* Plant Cell Physiol. **44:** 1368–1377.

Okazawa, A., Tang, L., Itoh, Y., Fukusaki, E., and Kobayashi, A. (2006). Characterization and subcellular localization of chlorophyllase from *Ginkgo biloba.* Z. Naturforsch. [C] **61:** 111–117.

Park, J.H., Oh, S.A., Kim, Y.H., Woo, H.R., and Nam, H.G. (1998). Differential expression of senescence-associated mRNAs during leaf senescence induced by different senescence-inducing factors in *Arabidopsis.* Plant Mol. Biol. **37:** 445–454.

Park, S.-Y., et al. (2007). The senescence-induced staygreen protein regulates chlorophyll degradation. Plant Cell **19:** 1649–1664.

Pei, J., Kim, B.-H., and Grishin, N.V. (2008). PROMALS3D: A tool for multiple protein sequence and structure alignments. Nucleic Acids Res. **36:** 2295–2300.

Porra, R.J. (1991). Recent advances and re-assessments in chlorophyll extraction and assay procedures for terrestrial, aquatic, and marine organisms, including recalcitrant algae. In Chlorophylls, H. Scheer, ed (Boca Raton, FL: CRC Press), pp. 31–57.

Pružinská, A., Anders, I., Aubry, S., Schenk, N., Tapernoux-Lüthi, E., Müller, T., Kräutler, B., and Hörtensteiner, S. (2007). In vivo participation of red chlorophyll catabolite reductase in chlorophyll breakdown. Plant Cell **19:** 369–387.

Pružinská, A., Anders, I., Tanner, G., Roca, M., and Hörtensteiner, S. (2003). Chlorophyll breakdown: Pheophorbide *a* oxygenase is a Rieske-type iron-sulfur protein, encoded by the *accelerated cell death 1* gene. Proc. Natl. Acad. Sci. USA **100:** 15259–15264.

Pružinská, A., Tanner, G., Aubry, S., Anders, I., Moser, S., Müller, T., Ongania, K.-H., Kräutler, B., Youn, J.-Y., Liljegren, S.J., and Hörtensteiner, S. (2005). Chlorophyll breakdown in senescent Arabidopsis leaves: Characterization of chlorophyll catabolites and of chlorophyll catabolic enzymes involved in the degreening reaction. Plant Physiol. **139:** 52–63.

Ren, G., An, K., Liao, Y., Zhou, X., Cao, Y., Zhao, H., Ge, X., and Kuai, B. (2007). Identification of a novel chloroplast protein AtNYE1 regulating chlorophyll degradation during leaf senescence in Arabidopsis. Plant Physiol. **144:** 1429–1441.

Reynolds, E.S. (1963). The use of lead citrate at high pH as an electron-opaque stain in electron microscopy. J. Cell Biol. **17:** 208–212.

Roca, M., James, J., Pružinská, A., Hörtensteiner, S., Thomas, H., and Ougham, H. (2004). Analysis of the chlorophyll catabolism pathway in leaves of an introgression senescence mutant of *Lolium temulentum.* Phytochemistry **65:** 1231–1238.

Rodoni, S., Mühlecker, W., Anderl, M., Kräutler, B., Moser, D., Thomas, H., Matile, P., and Hörtensteiner, S. (1997). Chlorophyll breakdown in senescent chloroplasts. Cleavage of pheophorbide *a* in two enzymic steps. Plant Physiol. **115:** 669–676.

Rosso, M.G., Li, Y., Strizhov, N., Reiss, B., Dekker, K., and Weisshaar, B. (2003). An *Arabidopsis thaliana* T-DNA mutagenized population (GABI-Kat) for flanking sequence tag-based reverse genetics. Plant Mol. Biol. **53:** 247–259.

Rüdiger, W. (2002). Biosynthesis of chlorophyll *b* and the chlorophyll cycle. Photosynth. Res. **74:** 187–193.

Sato, Y., Morita, R., Katsuma, S., Nishimura, M., Tanaka, A., and Kusaba, M. (2009). Two short-chain dehydrogenase/reductases, NON-YELLOW COLORING 1 and NYC1-LIKE, are required for chlorophyll *b* and light-harvesting complex II degradation during senescence in rice. Plant J. **57:** 120–131.

Sato, Y., Morita, R., Nishimura, M., Yamaguchi, H., and Kusaba, M. (2007). Mendel's green cotyledon gene encodes a positive regulator of the chlorophyll-degrading pathway. Proc. Natl. Acad. Sci. USA **104:** 14169–14174.

Schenk, N., Schelbert, S., Kanwischer, M., Goldschmidt, E.E., Dörmann, P., and Hörtensteiner, S. (2007). The chlorophyllases AtCLH1 and AtCLH2 are not essential for senescence-related chlorophyll breakdown in *Arabidopsis thaliana.* FEBS Lett. **581:** 5517–5525.

Schoch, S., Scheer, H., Schiff, J.A., Rüdiger, W., and Siegelman, H.W. (1981). Pyropheophytin *a* accompanies pheophytin *a* in darkened light grown cells of *Euglena.* Z. Naturforsch. [C] **36c:** 827–833.

Schoch, S., and Vielwerth, F.X. (1983). Chlorophyll degradation in senescent tobacco cell culture (*Nicotiana tabacum* var. "Samsun"). Z. Pflanzenphysiol. **110:** 309–317.

Seki, M., et al. (2002). Functional annotation of a full-length Arabidopsis cDNA collection. Science **296:** 141–145.

Shimokawa, K., Hashizume, A., and Shioi, Y. (1990). Pyropheophorbide *a*, a catabolite of ethylene-induced chlorophyll *a* degradation. Phytochemistry **29:** 2105–2106.

Shioi, Y., Tatsumi, Y., and Shimokawa, K. (1991). Enzymatic degradation of chlorophyll in *Chenopodium album.* Plant Cell Physiol. **32:** 87–93.

Smith, M.D., Schnell, D.J., Fitzpatrick, L., and Keegstra, K. (2002). In vitro analysis of chloroplast protein import. In Current Protocols in Cell Biology, J.S. Bonifacino, M. Dasso, J.B. Harford, J. Lippincott-Schwartz, and K.M. Yamada, eds (New York: Wiley Interscience), pp. 11.16.1–11.16.21.

Strain, H.H., Cope, B.T., and Svec, W.A. (1971). Analytical procedures for the isolation, identification, estimation and investigation of the chlorophylls. Methods Enzymol. **23:** 452–476.

Suzuki, T., Kunieda, T., Murai, F., Morioka, S., and Shioi, Y. (2005). Mg-dechelation activity in radish cotyledons with artificial and native substrates, Mg-chlorophyllin *a* and chlorophyllide *a.* Plant Physiol. Biochem. **43:** 459–464.

Takamiya, K., Tsuchiya, T., and Ohta, H. (2000). Degradation pathway (s) of chlorophyll: What has gene cloning revealed? Trends Plant Sci. **5:** 426–431.

Talavera, G., and Castresana, J. (2007). Improvement of phylogenies after removing divergent and ambiguously aligned blocks from protein sequence alignments. Syst. Biol. **56:** 564–577.

Tanaka, A., Ito, H., Tanaka, R., Tanaka, N.K., Yoshida, K., and Okada, K. (1998). Chlorophyll *a* oxygenase (*CAO*) is involved in chlorophyll *b* formation from chlorophyll *a.* Proc. Natl. Acad. Sci. USA **95:** 12719–12723.

Tanaka, R., Hirashima, M., Satoh, S., and Tanaka, A. (2003). The *Arabidopsis-accelerated cell death* gene *ACD1* is involved in oxygenation of pheophorbide *a*: Inhibition of pheophorbide *a* oxygenase activity does not lead to the "stay-green" phenotype in *Arabidopsis.* Plant Cell Physiol. **44:** 1266–1274.

Thomas, H. (1987). *Sid*: A Mendelian locus controlling thylakoid membrane disassembly in senescing leaves of *Festuca pratensis.* Theor. Appl. Genet. **73:** 551–555.

Thomas, H., and Hilditch, P. (1987). Metabolism of thylakoid membrane proteins during foliar senescence. In Plant Senescence: Its Biochemistry and Physiology, W.W. Thomson, E.A. Nothnagel, and R.C. Huffaker, eds (Rockville, MD: American Society of Plant Physiologists), pp. 114–122.

Thomas, H., and Howarth, C.J. (2000). Five ways to stay green. J. Exp. Bot. **51:** 329–337.

Tissier, A.F., Marillonnet, S., Klimyuk, V., Patel, K., Torres, M.A., Murphy, G., and Jones, J.D. (1999). Multiple independent defective *suppressor-mutator* transposon insertions in Arabidopsis: a tool for functional genomics. Plant Cell **11:** 1841–1852.

Tsuchiya, T., Ohta, H., Okawa, K., Iwamatsu, A., Shimada, H., Masuda, T., and Takamiya, K. (1999). Cloning of chlorophyllase,

the key enzyme in chlorophyll degradation: Finding of a lipase motif and the induction by methyl jasmonate. Proc. Natl. Acad. Sci. USA **96:** 15362–15367.

Vavilin, D., and Vermaas, W. (2007). Continuous chlorophyll degradation accompanied by chlorophyllide and phytol reutilization for chlorophyll synthesis in *Synechocystis* sp PCC 6803. Biochim. Biophys. Acta **1767:** 920–929.

Vicentini, F., Hörtensteiner, S., Schellenberg, M., Thomas, H., and Matile, P. (1995b). Chlorophyll breakdown in senescent leaves: identification of the biochemical lesion in a *stay-green* genotype of *Festuca pratensis* Huds. New Phytol. **129:** 247–252.

Vicentini, F., Iten, F., and Matile, P. (1995a). Development of an assay for Mg-dechelatase of oilseed rape cotyledons, using chlorophyllin as the substrate. Physiol. Plant. **94:** 57–63.

Vidi, P.A., Kanwischer, M., Baginsky, S., Austin, J.R., Csucs, G., Dörmann, P., Kessler, F., and Brehelin, C. (2006). Tocopherol cyclase (VTE1) localization and vitamin E accumulation in chloroplast plastoglobule lipoprotein particles. J. Biol. Chem. **281:** 11225–11234.

Willstätter, R., and Stoll, A. (1913). Die Wirkungen der Chlorophyllase. In Untersuchungen über Chlorophyll, R. Willstätter and A. Stoll, eds (Berlin: Verlag Julius Springer), pp. 172–187.

Wüthrich, K.L., Bovet, L., Hunziker, P.E., Donnison, I.S., and Hörtensteiner, S. (2000). Molecular cloning, functional expression and characterisation of RCC reductase involved in chlorophyll catabolism. Plant J. **21:** 189–198.

Ytterberg, A.J., Peltier, J.B., and van Wijk, K.J. (2006). Protein profiling of plastoglobules in chloroplasts and chromoplasts. A surprising site for differential accumulation of metabolic enzymes. Plant Physiol. **140:** 984–997.

Ziegler, R., Blaheta, A., Guha, N., and Schönegge, B. (1988). Enzymatic formation of pheophorbide and pyropheophorbide during chlorophyll degradation in a mutant of *Chlorella fusca* SHIRIA et KRAUS. J. Plant Physiol. **132:** 327–332.

Zimmermann, P., Hirsch-Hoffmann, M., Hennig, L., and Gruissem, W. (2004). GENEVESTIGATOR. Arabidopsis microarray database and analysis toolbox. Plant Physiol. **136:** 2621–2632.